The human blood harbors a phageome which differs in Crohn's disease

Quentin LAMY-BESNIER[1,2], Ilias THEODOROU[1], Maud BILLAUD[1], Hao ZHANG[1], Loïc BROT[2], Antoine CULOT[3], Guillaume ABRIAT[3], Harry SOKOL[1,2,4,5], Marianne DE PAEPE[1], Marie-Agnès PETIT[1,*], and Luisa DE SORDI[2,5,*]

[1] Université Paris-Saclay, INRAE, AgroParisTech, MICALIS Unit, 78352 Jouy en Josas, France

[2] Sorbonne Université, INSERM, Centre de Recherche Saint-Antoine, 75012 Paris, France

[3] Rime Bioinformatics SAS, Palaiseau, France

[4] AP-HP, Saint Antoine Hospital, Gastroenterology Department, 75012 Paris, France.

[5] Paris Center for Microbiome Medicine (PaCeMM) FHU, Paris, France

[*] Correspondence: luisa.de_sordi@sorbonne-universite.fr (L.D.S.), marie-agnes.petit@inrae.fr (M.A.P.)

Running title

Blood phageome in Crohn's disease

Keywords

Virome; bacteriophage; phage; metagenomics; gut virome

Abstract

Increasing evidence suggests that the human blood hosts microbes including bacteria and eukaryotic viruses, which could have important implications for health. Bacteriophages of the blood are challenging to study and have been overlooked, but could translocate to this environment from different body-sites. We thus developed specific virome protocols and analysis methods to study the viral communities of blood samples obtained from healthy individuals and Crohn's disease (CD) patients. We uncovered a diverse viral community in the human blood, dominated by phages infecting Pseudomonadota bacteria. We found that an important fraction of those phages overlaps with the gut virome, consolidating the idea that gut phages can translocate to the blood. Strikingly, viral communities of the blood were different between CD patients and healthy individuals, revealing a new signature of disease. This was not the case for fecal viral communities. Collectively, these results advance our knowledge of the microorganisms present in the human blood and pave the way for further studies of this environment in the context of disease.

Introduction

Despite being initially thought to be sterile, increasing evidence shows that the human blood contains bacteria[1–5], although they do not form a common community across individuals[6]. The blood also hosts viruses, but efforts have been mainly directed at identifying eukaryotic viruses, overlooking bacterial viruses, bacteriophages (phages)[7–10]. Phages are important members of human-associated microbiota, particularly in the gastrointestinal tract (GIT) where they have been linked to a variety of diseases[11–14]. Their entry into the blood has also been suggested by studies showing the translocation of phages across intestinal cell layers *in vitro*[15,16]. Therefore, it is possible that a community of phages exists in the blood and could be relevant to human health. Recently, the sequencing of circulating DNA in a human cohort of sepsis revealed a blood phageome that could be employed to identify the pathogens causing the infection[17]. These findings underscore the significant potential of blood phage communities, and call for further studies characterizing the encapsidated and circulating viral particles of the human blood phageome to fully leverage its possibilities as a marker of disease.

The limited number of studies on blood microbes can be explained by very low concentrations of microorganisms, which is a challenge for typical metagenomic experimental and analytical approaches. The issue is exacerbated for viruses having small genomes, like phages, resulting in small quantities of total DNA that are hardly compatible with metagenomic sequencing approaches. Contamination of the samples by environmental DNA is also a particular concern in this context. A keystone study used over 8,000 human blood samples to identify multiple viruses, including prevalent human herpesviruses and phages, but could not discriminate contamination from reliable signals[18]. This study and most others used only total DNA, as opposed to performing a size filtration to remove bacteria from the samples (virome sequencing), which led to reduced relative abundances of viruses. Novel and virus-focused studies are thus required for the reliable and accurate exploration of the human blood virome.

Crohn's disease (CD) is a chronic, inflammatory bowel disease characterized by recurrent inflammation of the GIT. Despite ever-increasing worldwide incidence, no specific marker of this complex disease has been identified[19]. On top of genetic and environmental causes, the gut microbiota composition has been strongly associated with CD[20–22]. However, this signature becomes blurred when the analysis is restricted to the viral fraction of the microbiota. Initially, the gut virome was found to be correlated with CD[23–25], but nowadays it is no longer considered linked with the disease due to its intrinsically high interindividual variability[26]. This variability is driven by the broad diversity of the gut virome. Therefore, in order to investigate the potential link between the human virome and CD, other viral communities with a reduced complexity might be more appropriate.

Here, we developed a specific experimental and bioinformatic approach to address the challenges of the blood environment in order to characterize the human blood virome. Using this method on a cohort comprised of healthy and CD individuals, we first show that the blood

virome is essentially composed of a diverse community of phages infecting mostly bacteria of the Pseudomonadota phylum (previously known as Proteobacteria). In order to explore the origins of these phages, we took advantage of fecal samples obtained from the same individuals, as well as of databases of gut and oral viruses. We found that the gut virome was an important source of blood phages. Remarkably, the comparison of healthy and CD individuals uncovered a difference in the blood virome composition, whereas no such distinction was observed in the fecal virome. Among the differentially abundant phages, all of those that are less abundant in CD patients infect the genus *Acinetobacter*, which marks a first step towards unravelling the connection between CD and the blood virome. These data provide the first comprehensive overview of the human blood phageome and underline its potential to better understand complex diseases such as CD.

Results

Accurate determination of vOTUs in blood and fecal samples

To study their viral communities, we collected blood and fecal samples from 15 CD patients and 14 healthy individuals (**Fig. 1A** and **Table S1**). Since blood samples contain low amounts of DNA and are prone to contamination[18,27], we set up two negative controls consisting of a blood collection tube and a standard microtube, both filled with sterile double-distilled water before processing. Viral DNA was enriched from all samples, prepared and sequenced (Methods and **Table S2**). We developed a specific pipeline for the analysis of these samples (**Fig. 1B-C**). After cleaning and removing the human reads, an assembly was performed for each individual, as well as using all the samples together (cross-assembly), leading to a total of 165,933 contigs larger than 2 kb. The contigs were clustered at the species level, reducing the number of operational taxonomic units (OTUs) to 85,985. To select viral OTUs (vOTUs), we used a combination of dedicated tools and viral databases (Methods), detecting a total of 17,454 vOTUs (**Fig. S1A-B-C**). The quality of vOTUs was assessed using CheckV[28] (**Fig. S2A-B**). These vOTUs were then characterized through annotation, host prediction and classification. The sequence and annotation of all vOTUs are publicly available, and complete information for each vOTU can be found in **Table S3**.

The blood being an environment characterized by a low abundance of viruses, we used a stringent filter to only consider OTUs for which sufficient evidence for their presence in each sample was achieved. These criteria were such that on average, each nucleotide of the OTU must be sequenced at least once (depth ≥ 1), and at least 50% of the OTU should be sequenced (coverage ≥ 50%). Only the OTUs passing these criteria were considered as present in a given sample. On average, this led to the removal of 80% OTUs per sample, which had few reads mapped to them but not sufficiently (**Fig. S3A**).

Next, to identify and remove contaminant OTUs from our samples, the content of negative control samples was determined. This analysis revealed a high number of contaminants (total of 7,764 OTUs), and a surprising difference between the microtube and the blood collection tube, with the latter being much richer in contaminants (**Fig. 1D**). This highlights the importance of the adequate choice of controls in metagenomics studies. When looking at the classification of these OTUs, bacterial contamination dominated (6,047 OTUs), followed by viral (484 OTUs) and eukaryotic (438 OTUs) sequences (**Fig. S4A**). Both tubes were heavily contaminated with DNA from microbes associated with the skin microbiota: bacteria belonging to the Actinomycetota phylum, including families such as *Proprionibacteria*, as well as phages predicted to infect such hosts, and yeasts from the genus *Malassezia* (**Fig. S4B-C-D)**. This suggests that microorganisms from the human skin are responsible for an important part of the contamination. A core of contaminant sequences was found across the blood samples, showing that the contaminants are not tube-specific and were appropriately identified using our two negative controls (**Fig. S5**). We favoured a stringent approach and removed all the OTUs present in any of these two negative controls. This filtering step led to

the loss of an average of 57% of the reads for the blood samples, and 4% for the fecal samples (**Fig. S3B**).

Viromes usually contain a portion of non-viral DNA, which in our case represented on average 83% of the reads in blood samples and 23% in fecal samples (**Fig. S3C**). This fraction consisted mostly of bacterial DNA (**Fig. S6A-B-C**) and was also removed. Finally, non-contaminant vOTUs represented around 6% of the reads for the blood (**Fig. 1E**), highlighting the importance of the filtering steps. As expected, these filters had a small impact on the fecal samples, with an average of 75% of reads per sample kept. Non-contaminant vOTUs were significantly less abundant in the blood of CD patients, compared to healthy individuals. However, this did not translate in a lower number of viral particles in the CD blood samples, as determined by spiking (Fig. S11A). Moreover, the opposite trend was observed for the fecal samples.

By designing an adequate and conservative pipeline, we thus have access to the viral composition of each sample with high confidence.

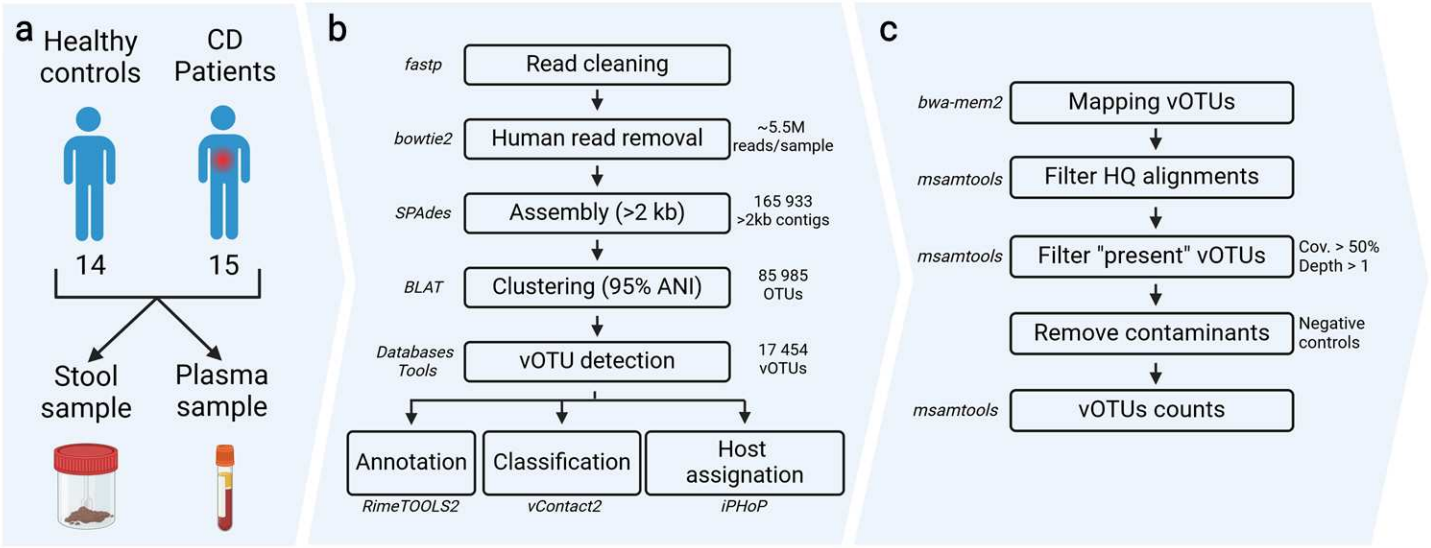

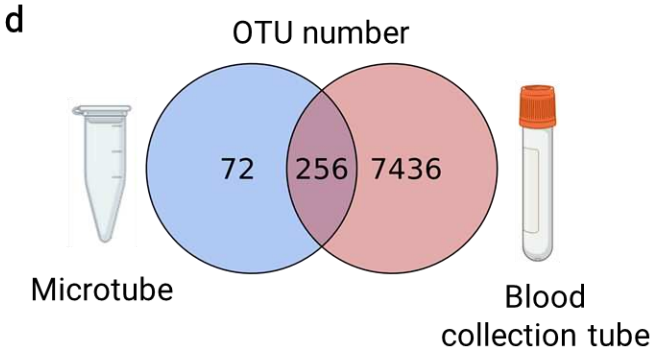

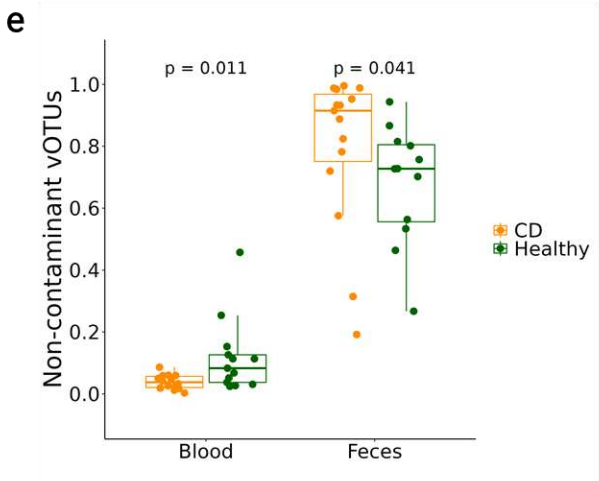

Figure 1: Determination of the human blood virome.
a. Schematics of the cohort and sample collection. **b.** Bioinformatic pipeline for the detection of vOTUs. **c.** Bioinformatic pipeline for the determination of vOTU counts. **d.** Number of OTUs in the two negative control samples. **e.** Relative abundance of the non-contaminant (i.e. not found in the negative control samples) vOTUs per sample type and disease status (orange = CD patients, green = healthy individuals).

The human blood virome is diverse and dominated by phages infecting Pseudomonadota

Blood samples carried a median of 132 vOTUs, for a total of 1,794 unique vOTUs present across the 27 samples, demonstrating that the human blood virome contains a diverse viral community (**Fig. 2A**). The spiking of human samples with two phages, SPP1 (dsDNA) and M13 (ssDNA), led to estimating that around 10^5 viral particles are present per mL of blood (**Fig. 2B**). This is the first attempt at quantifying the number of viral particles in the blood virome. Altogether, these results converge on the presence of a relatively large community of viruses in the blood.

We then characterized the nature of this human blood virome. Firstly, we were able to detect eukaryotic viruses previously reported to be frequent in human blood, mainly Anelloviruses[7,10] (**Fig. S7**). Interestingly, Herpesviruses, which are also frequently reported in the human blood[8,9,18] were found in some blood samples but also in the negative controls, so their natural presence in this ecosystem cannot be ascertained. However, phages largely dominated the viral community of the human blood. This phageome was mostly composed of phages infecting Pseudomonadota bacteria (> 80% relative abundance), followed by phages infecting bacteria from the phyla Bacillota (formerly known as Firmicutes), Bacteroidota (formerly Bacteroidetes) and Actinomycetota (**Fig. 2C**). This is in line with the main bacterial phyla found in the human blood[1–3,5], as well as with other human-associated microbiota. Another significant characteristic of viral communities is their lifestyles, which can be classified as either virulent, where viruses lyse their host to release progeny, or temperate, where viruses can integrate into the host chromosome as prophages and replicate passively. By looking at the presence of integrase genes in high-quality or complete vOTUs, we estimated that around ~20% of the blood high-quality vOTUs were temperate (**Fig. 2D**), and they collectively represented 20% of the high quality vOTUs abundances (**Fig. S8A**). Taking these well-assembled vOTUs as a proxy for the whole community, we predict that temperate phages should represent collectively ~20% of the blood viral community.

Collectively, we uncover a diverse viral community in the human blood, dominated by phages infecting mostly Pseudomonadota bacteria.

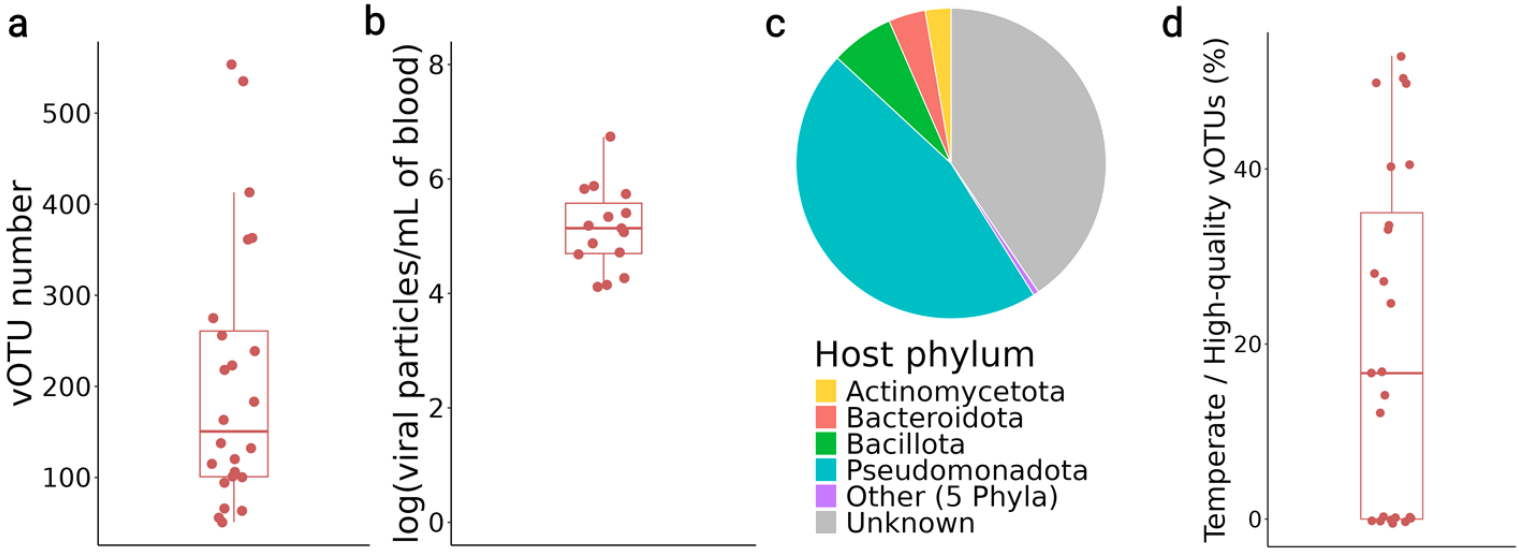

Figure 2: Overview of the human blood virome.
a. Number of vOTUs per blood sample. **b.** Estimated number of viral particles per mL of blood and per blood sample. **c.** Distribution of the predicted host phyla for all the vOTUs found in blood samples. **d.** Percentage of vOTUs with a temperate lifestyle among the high-quality vOTUs. The temperate lifestyle was predicted by the presence of genes coding for an integrase, and only the high-quality vOTUs were considered (Methods).

Origins of the human blood virome

Two main hypotheses could explain the presence of phages in the human blood: induction of prophages integrated in blood bacteria, or translocation from other body-sites. As most phages were classified as virulent (**Fig. 2D**), induction does not seem prevalent, which prompted us to explore the second option. Bacteria are able to translocate through the intestinal epithelium in both physiological and disease conditions[29], and reports have also shown that phages translocate through human cells *in vitro*[16]. The intestinal microbiota also harbors the highest virus density, making the gut virome the most probable origin of blood phages.

It is to investigate this hypothesis that we sequenced fecal samples collected from the same individuals, and at the same time as the blood samples. Their analysis revealed typical characteristics of the human gut virome, which illustrates the reliability of our analysis pipeline. In particular, we found a median of 722 vOTUs per fecal sample (**Fig. S9A**), for a total of 10^8-10^9 viral particles per gram of feces (**Fig. S9B**), with predicted infected hosts being mainly Bacteroidota and Bacillota bacteria (**Fig. S9C**), and an estimation of around 50% of temperate phages based on high-quality vOTUs (**Fig. S9D** and **Fig. S8B**). When comparing the vOTUs present in the blood to those present in the fecal samples, only ~3% of blood vOTUs overlapped, representing ~1.5% of vOTUs per sample and a corresponding ~1.5% of abundance (**Fig. 3A-B** and **Fig. S10A**). A detailed study of these shared vOTUs is included in a dedicated, parallel article where we looked at the nature of viruses that could translocate

from the gut to the bloodstream. To complement this analysis, we broadened the search for gut phages in the blood virome by comparing our blood vOTUs with recently released databases of gut viruses [30–34]. This resulted in ~20% of blood vOTUs having homology (>90% identity over >90% target length) with gut phages (**Fig. 3C**), representing ~20% of the relative abundance of blood viruses (**Fig. S10B**). This suggests that the gut is indeed an important source for the blood virome, although it does not account for the majority of blood phages. It also illustrates the value of leveraging large databases built from samples collected at multiple sections of the GIT, as opposed to our limited number of samples of fecal origin.

In an attempt to find the origin of the remaining 80% blood viruses, we interrogated the database of viruses found at another body-site from which phages could translocate: the mouth. The oral microbiota contains an important fraction of Pseudomonadota bacteria[35]. As this phylum hosts most of our blood phages, the mouth appears to be relevant candidate. We thus compared the blood vOTUs with viruses from the Oral Virus Database[36]. We found ~2% of blood vOTUs with high similarity to oral phages (>90% identity over >90% target length), which together represented ~2% of relative abundance (**Fig. 3D** and **Fig. S10C**), showing that the oral virome also contributes to the blood virome.

Altogether, while the origins of the blood virome are difficult to establish, the present analysis suggests that the gut virome is an important contributor.

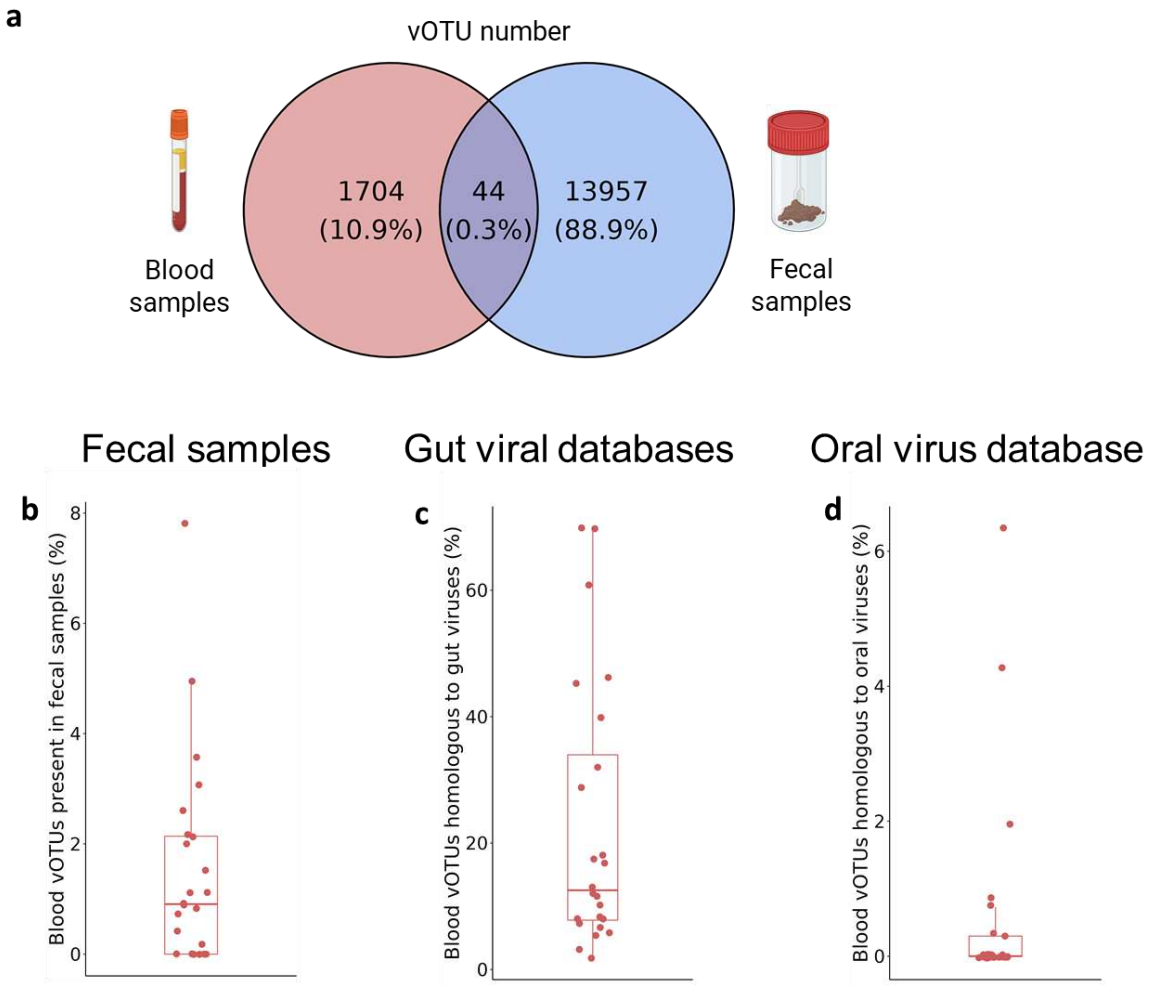

Figure 3: The origins of the human blood virome.
a. Venn diagram of the vOTUs identified in blood and fecal samples. **b.** Percentage per blood sample of vOTUs that are also found in fecal samples. **c.** Percentage per blood sample of vOTUs that have a close homolog in a gut viral database. **d.** Percentage per blood sample of vOTUs that are have a close homolog in the Oral Virus Database.

The blood virome differs in Crohn's disease

We then proceeded to compare the blood viral community between healthy individuals and CD patients (**Fig. 4A**). Most of the metrics presented previously, such as the proportion of temperate phages or the number of viral particles per mL, did not differ between the two groups (**Fig. S11A-B**). Instead, we found a difference in the host phyla that the vOTU are predicted infect: CD blood viromes presented an increase in phages infecting Bacteroidota (p=0.03) (**Fig. S11C**). This phylum is similarly increased in the gut microbiota of CD patients[37], suggesting that changes in the blood virome may be linked to those in the gut bacteriome.

We also compared the alpha-diversity between both groups, measured by the Shannon index, and did not find any significant differences (**Fig. 4B**). Similar observations were made with other diversity metrics, including richness as well as Simpson and Chao1 indexes (**Fig. S12A-B-C**). However, comparing the composition of both communities through an analysis of beta-diversity revealed a strong difference between the two groups (Bray-Curtis dissimilarity, p=0.001, **Fig. 4C**). While the healthy group displayed essentially a scattered distribution, the CD blood samples clustered together. These results were confirmed using the Jaccard index (p=0.001, **Fig. S12D**) and indicate that the blood virome harbors a signature of CD.

Furthermore, when the same analysis was performed with fecal samples (**Fig. 4D**), we did not observe any major changes in the viral communities (**Fig. S11D-E-F**). One of the main shifts observed in the gut microbiota of CD patients is a reduction of the species *Faecalibacterium prausnitzii*[20,21]. We saw a comparable diminution of the relative abundance of phages infecting the *Faecalibacterium* genus in CD patients (p=0.012, **Fig. S11G**), suggesting similar changes in the gut bacteriome and virome. More generally, a slight decrease in viral diversity in the fecal samples of CD patients was identified (p=0.0074), which could be due to the reduced bacterial diversity associated with CD (**Fig. 4E** and **Fig. S12E-F-G**). Importantly, the two groups are not separated in terms of beta-diversity (**Fig. 4F** and **Fig. S12H**). This can be explained by inter-individual variability of the gut virome which has been shown to hinder attempts at finding disease signals with metagenomic approaches[26].

Taken together, our results suggest that the blood virome is more discriminant for CD than the gut virome.

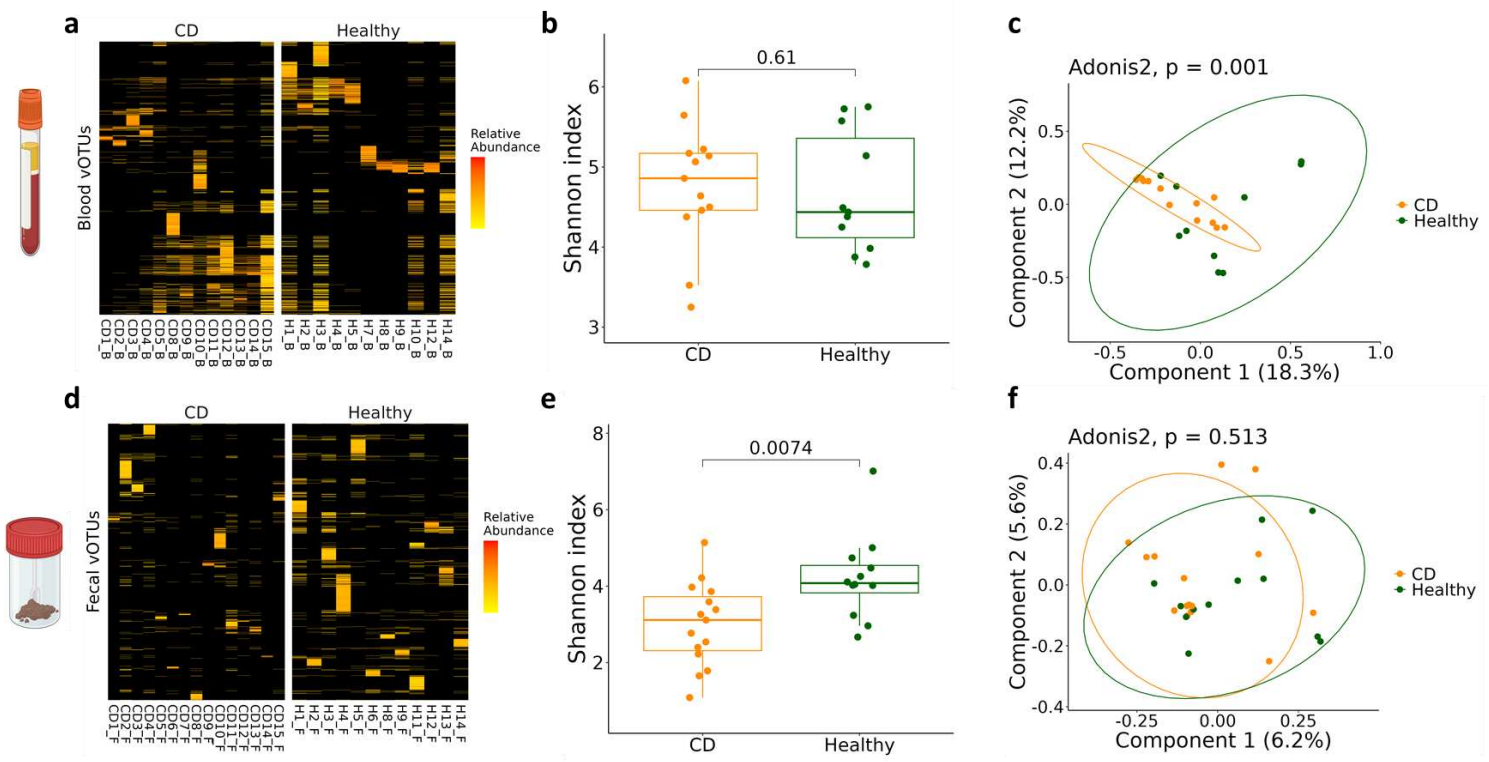

Figure 4: Differences between healthy individuals and CD patients in blood and fecal communities.

a. Heatmap of the relative abundance of blood vOTUs across blood samples, separated by disease status. **b.** Alpha diversity of the blood samples measured by the Shannon index and separated by disease status. **c.** PCoA of the vOTU composition of the blood samples, using the Bray-Curtis dissimilarity distances. The associated Adonis2 analysis revealed a significant difference between both groups (p=0.001). **d.** Heatmap of the relative abundance of fecal vOTUs across fecal samples, separated by disease status. **e.** Alpha diversity of the fecal samples measured by the Shannon index and separated by disease status. **f.** PCoA of the vOTU composition of the fecal samples, using the Bray-Curtis dissimilarity distances. The associated Adonis2 analysis revealed no significant difference between both groups (p=0.513).

Acinetobacter-infecting phages are depleted in CD individuals

In order to uncover which phages could be responsible for this different blood viral community in CD, we then performed a differential analysis. A total of 46 differentially abundant vOTUs were identified (**Fig. 5**), which consolidates the difference between the blood viral communities of healthy and diseased individuals. In contrast, the same analysis run on the fecal samples did not reveal any differentially abundant vOTUs, being in line with the lack of difference observed by beta-diversity metrics. Among the differentially abundant blood vOTUs, 27 were enriched in CD patients, while 19 showed increased abundance in healthy individuals. While the 27 vOTUs more abundant in CD patients had a variety of predicted hosts, with mostly Pseudomonadota and few Bacillota bacteria, a striking pattern emerged for the

19 vOTUs more abundant in healthy individuals, which were all infecting bacteria from the genus *Acinetobacter*. These results suggest that the changes of the blood virome associated with CD have a precise effect on the healthy blood virome, reducing the population of phages infecting *Acinetobacter* while promoting the presence of a variety of other phages without a clear pattern. Around 15-20% of the differentially abundant phages were temperate, for both the over- and under-represented vOTUs (using vOTUs of all qualities in this case), showing that prophage induction does not explain the changes in the blood virome of the CD patients.

To conclude, while a variety of phages are more abundant in the blood of CD patients, only the phages infecting Acinetobacter are found to be lower in numbers.

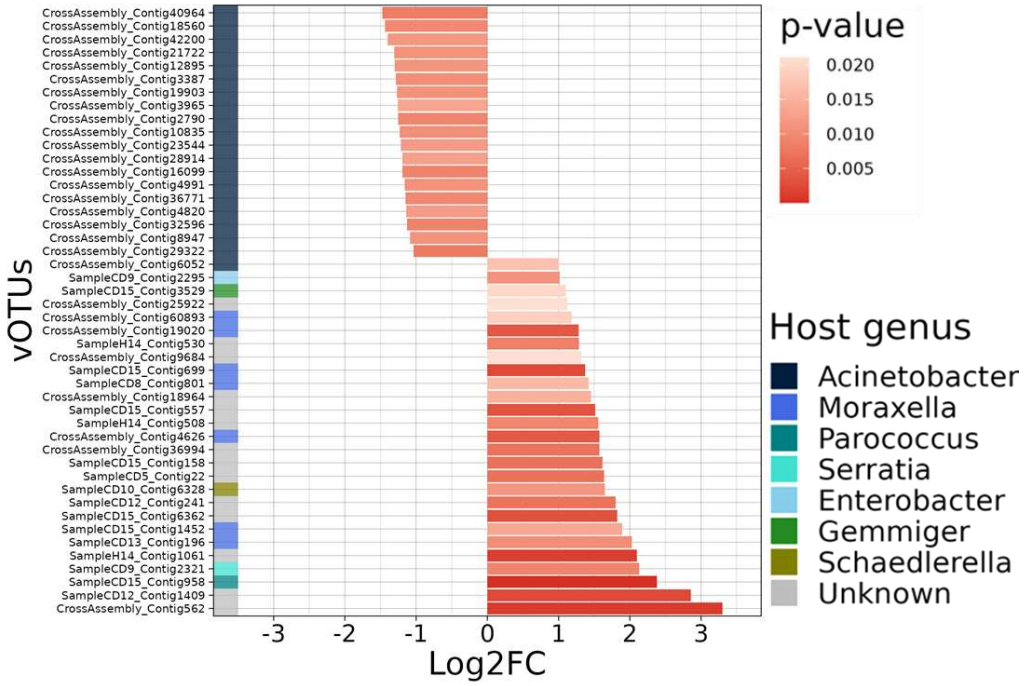

Figure 5: Differentially abundant blood vOTUs.
Differential analysis was performed using Maaslin2. Only vOTUs with a q-value < 0.25 and Log2FC > 1 or < -1 were considered significant and are displayed.

Discussion

The viral component of the human blood remains largely unexplored, despite its vast potential as a marker of disease. This has been highlighted by recent studies showing that circulating phage DNA can be used to precisely identify bacterial pathogens causing sepsis[17] or that the presence of specific phages in hemocultures could help detect pathogens[38]. In this study, we developed adequate methods to uncover a diverse phage community in the human blood. Most of the blood phages were predicted to infect Pseudomonadota bacteria, mirroring blood bacteria, dominated by the same phylum[1–3]. Recent microbiota studies have shown that the phage composition usually reflects the bacterial composition, as both populations co-exist over long periods of time[39]. Our observations follow this trend, which explains the dominance of phages infecting this phylum in this ecosystem. We additionally report the first quantification of viral particles in human blood, estimated at 10^5 viral particles per mL of blood. Since the number of bacterial genomes predicted by 16S sequencing is around 10^6 per mL[4,40], the hypothetical phage:bacteria ratio of 1:10 in the blood matches the one reported in the human gut[41], suggesting a similar organization.

However, despite the unexpected diversity and abundance of phages in the human blood we uncover, key questions remain about their impact on this ecosystem. With our virome sequencing approach, we are unable to distinguish infectious from inactive phage particles. Phage predation of blood bacteria is therefore difficult to assess with our data. The blood environment is known to affect phage-bacteria interactions and to reduce phage infectivity in some cases[42,43], though large-scale studies are lacking to confirm these observations. This suggests that phages would not be able to replicate in this environment. The fact that bacteria isolated from the blood are in L-form or dormant metabolic states[2,4] is another hindrance limiting phage replication in the blood. The presence of a blood phage community is therefore likely to have a limited effect on blood bacteria. Yet, such phages could have a direct impact on the human host, as exemplified through increasing examples of interactions between phages and the immune system[44–46], including in the case of CD where ileal viromes of patients were found to exacerbate inflammation *in vivo*[47]. A phage infecting *Ralstonia* bacteria (Pseudomonadota phylum) was recently isolated from the blood and was shown to be persistent in this environment[48], which is in line with our results. Remarkably, this phage codes for proteins which are capable to be expressed in eukaryotic cells and transported into the nucleus, pointing out the possible interactions between blood phages and the human host. We also observed significant variations in the blood virome composition between CD and healthy individuals, which could reflect interactions between blood viruses and the immune system, given that CD strongly affects the immune response. More generally, in tandem with eukaryotic viruses such as Anelloviruses, phages could play a role in the regulation of the immune system, as observed in the gut microbiota[49–51]. Altogether, much like for bacteria, the presence of phages in the blood could have important implications for human health, but remains to be better understood.

Another central interrogation is about the origin of the blood phages. Given that phage half-life in blood has been estimated to few hours in pharmacokinetics studies[52], and with phage replication expected to be negligible in this environment, phage input must be constant and quantitatively high to match our observations. Prophage induction is likely not strongly contributing to the presence of phage particles in the blood, as we estimate that temperate phages do not constitute the majority of the community. Additionally, bacterial metabolism is also expected to be minimal in the blood environment and would prevent virion production. Instead, we suggest that the major contributor would be translocation from different body-sites. Translocation of phages across intestinal epithelial cells has been demonstrated *in vitro*[16], and these findings are consolidated by the results of our parallel paper, demonstrating phage translocation across intestinal and endothelial cell layers, as well as *ex vivo* across murine intestinal tissues. This provides a potential mechanism for a gut origin of blood viruses. In the present report, we found that the gut virome is a notable and significant source of blood phages, with around 20% of blood phages homologous to gut phages. Likewise, studies focusing on the bacteria of the human blood found that the gut microbiota is an important source of blood bacteria, with bacterial translocation as an underlying mechanism[1,3,5]. Notably, only 3% of blood viruses were found in paired fecal samples. A tentative explanation could be that the fecal microbiota is not representative of the microbiota found at all sites of the GIT[53], while phage translocation may happen throughout its different sections, according to their different permeability. In particular, the small intestine is known for its high prevalence of Pseudomonadota bacteria[53,54], which corresponds to the most frequent host phylum of blood phages. Therefore, its higher permeability, compared with the large intestine[55], could explain the prevalence of phages infecting this phylum in the blood, and their scarceness in faecal samples. While some of the gut viral databases include other types of samples, fecal samples largely dominate and the inclusion of more viruses from other sections of the GIT would probably improve our search for the origin of blood phages. Nonetheless, the origin of a large part of blood viruses remains unknown. We have identified a limited contribution from the oral virome, which may become more substantial as oral virus databases expand to match the richness of intestinal ones (around 170,000 viral species in our combination of gut databases compared to less than 50,000 in the Oral Virus Database), thereby enhancing our understanding of their connection to this ecosystem.

Other human-associated microbiota could also be explored to better understand the origin of blood phages. The skin hosts a well-known microbial community of yeasts, bacteria and phages[56]. However, the bulk of the organisms identified in the negative control samples was constituted of members of the skin microbiota such as *Malassezia* yeasts, *Propionibacterium* or other Actinomycetota bacteria, as well as their viruses. To ensure the reliability of our study, all these organisms were removed, which limits our ability to then detect skin viruses in our analysis. Nevertheless, the likelihood of viruses translocating through the skin appears to be low due to its stratified layers, including compact keratinocytes, and relatively low vascularity. Another more promising candidate could be the lung microbiota, which possesses a thin epithelium that facilitates gas exchanges and which could allow virus translocation. Lung

epithelial cells were actually found to have the highest phage uptake in a study comparing seven different cell types[15], highlighting the permeability of the lung epithelium and making the lungs a likely source of blood phages. Unfortunately, no database of lung viruses exists to date. The characterization of the viruses of this environment is ongoing[57], which should enable to investigate its promising relation with the blood virome in the near future.

CD has been extensively studied in relation to the gut microbiota. Despite the lack of a specific marker of CD, significant changes in the gut microbiota of CD patients have been uncovered[20–22]. While earlier studies suggested similar changes in the gut virome[23–25], recent analysis shows no significant differences between CD patients and healthy individuals[26]. Despite noting a decrease in viral alpha diversity among CD patients, which parallels the reduced bacterial diversity in this population, our observations also did not reveal significant disparities in the overall community composition. These findings therefore support the idea that the gut virome cannot be a marker of CD. The challenge most likely stems from the significant complexity and interindividual variability of this viral community[41], making it difficult to identify a unified signal of disease.

Conversely, microbial communities outside of the gut tend to exhibit less complexity, which could facilitate the identification of a CD-specific signal. We thus chose the blood virome, which contains few viruses and is still unexplored. Our findings reveal for the first time an association between blood virome and a non-infectious disease. CD causes a myriad of changes in the immune status of the patients, as reflected by increases in inflammatory markers routinely measured in the blood such as the C-reactive protein. How these alterations of the immune system can in turn affect the phage population remain difficult to predict. Besides, CD is also known to undermine the gut barrier integrity and thus its permeability, which could lead to changes in phage transfer to the blood. In a parallel article, we show that viruses are more frequently found in both fecal and blood samples of the same individual for CD patients. This confirms the increased transfer of gut phages into the blood in CD, potentially underpinning the changes in the blood virome observed in CD patients. Other studies have reported associations between blood bacterial communities and diseases affecting the immune system, such as IgA nephropathy[40] or acute pancreatitis[3]. Our work further reinforces the nascent link between blood microbes and disease by integrating the viral component.

We were able to precisely identify a group of differentially abundant phages in CD patients. Strikingly, all the underrepresented phages had *Acinetobacter* as predicted host. This constitutes a clear signal of the effect of CD on blood viral communities and establishes a novel signature of disease. *Acinetobacter* has been reported to be one of the most represented bacterial genera found in the blood in multiple studies, with relative abundances from 3 to 10%[3–5]. Changes in the population of phages infecting this genus could therefore have strong implications on this ecosystem. If the virome reflects the bacteriome, one could expect that the abundance of the bacteria is likewise reduced in the blood of CD patients. Nevertheless, current knowledge of blood bacteria is limited and further work, such as sequencing both

bacterial and viral DNA of blood samples, is required to better understand of the significance of this promising observation.

To conclude, our results uncover unsuspected phage diversity in the blood virome, advancing our understanding of this environment. This led to the identification of a different blood viral community in CD patients, which could be used as a signature of CD and improves our comprehension of this complex disease. Altogether, our findings pave the way for further exploration of the virome and microbiome of the blood in context of other disorders.

Material and Methods

Cohort

CD patients and healthy individuals were recruited through the Gastroenterology Department of the Saint-Antoine Hospital (Paris, France). All patients provided their informed consent, and the study was approved by the corresponding ethics committee (Comité de Protection des Personnes Ile-de-France IV, IRB 00003835 Suivithèque study; registration number 2012/05NICB). Our cohort contained 15 CD patients and 14 healthy controls. None of the individuals underwent intestinal surgery, and none took any antibiotic treatment in the last 3 months before sample collection. The median age of the cohort was of 38 ± 11 years. Detailed information about all the individuals of the cohort can be found in **Table S1**.

Sample collection

Comparing serum and plasma for the retrieval of phages (samples were spiked with T4, lambda and M13 phages) showed no major difference. Therefore, plasma was chosen for its easier downstream processing. Blood was collected in blood collection tubes designed for plasma collection (Dutscher ref. 369032), and immediately put on ice upon drawing. The samples were then centrifuged at 2,000 g for 10 min to separate the plasma. Plasma was then filtered through a 0.45 µm cellulose acetate filter, and stored at -20°C.

Fecal samples were collected directly in RNAlater (Sigma ref. R0901) and homogenized by vortexing using glass beads (Sigma ref. Z265942). After a centrifugation at 20,000 g for 15 min at 4°C, the supernatant was removed, and the pellet was directly stored at -80°C. RNAlater contains a high concentration of ammonium acetate, which precipitates phages particles. Phages are therefore contained in the pellet after centrifugation. Blood and fecal samples from the same individual were collected on the same day.

For negative controls, a blood collection tube and a low-binding Eppendorf tube (ref. EP0030108426) containing sterile, double-distilled water were used.

Viral DNA preparation and sequencing

To extract the viral DNA from blood and fecal samples, we adapted a virome protocol from Billaud *et al*[58]. Fecal samples (0.2 g) were thawed on ice, resuspended in 7 mL of Tris 10 mM pH 7.5. Plasma samples (3 mL) were thawed on ice. After this step, all samples were processed similarly. First, the samples were centrifuged at 4,750 g for 10 min at 4°C to remove most bacterial cells. The supernatant was then filtered through a 0.45 µm PES membrane filter to remove remaining bacteria. At this step, samples were spiked with known quantities of phages SPP1 (dsDNA) and M13 (ssDNA) (see "Estimation of the number of viral particles in samples by spiking" section). The negative control samples were not spiked. A benzonase-nuclease treatment (250 U, Sigma ref. E1014) was then performed for 2h at 37°C. In order to concentrate viruses, samples were mixed with 0.5 M NaCl and 10% weight/volume PEG-8000, followed by overnight incubation at 4°C. Samples were then centrifuged at 4,750 g for 30 min

at 4°C. The precipitate was collected and re-suspended in 400 µL Tris 10 mM pH 7.5, and shaken gently with an equal volume of chloroform in order to kill remaining bacteria and reduce vesicle contamination. After transferring in Maxtract gel tubes (Qiagen ref. 129056), the samples were centrifuged at 16,000g for 5 min at 4°C, after which the aqueous phase was extracted. To remove non-encaspidated DNA, samples were treated with TURBO DNAse I (8 U, ThermoFisher ref. AM2238,) and RNAseI (20 U, ThermoFisher ref. EN0601). DNAse was then inactivated using EDTA at a final concentration of 20 mM. To break open the capsids, proteinase K was added (40 µg) with 20 µL of SDS 10% before incubation at 56°C for 3 h. The samples were transferred into Maxtract gel tubes containing an equal volume of Phenol-Chloroform-Isoamyl alcohol (25:24:1, ThermoFisher). After vigorous vortexing, samples were centrifugated at 16,000 g for 5 min at 4°C. The aqueous phase was extracted and transferred to a new Maxtract gel tube. To remove phenol traces, chloroform/isoamyl alcohol (24:1, ThermoFisher) was added, followed by another identical centrifugation. The aqueous phase was extracted and DNA precipitated using sodium acetate (0.3 M), ethanol (2.5 volumes) and glycogen (20 µg/mL final concentration), then incubated 1 h at -20°C. The samples were then centrifuged at 16 000 g, 30 min, 4°C. The pellet was washed twice with 0.5 mL cold 75% ethanol. After ethanol removal, the dry pellet was resuspended in Tris 10 mM pH 8 and stored at -20°C.

Libraries were then prepared using the xGen kit, which provides a step to convert ssDNA to dsDNA with minimal biais[59]. The resulting libraries were then sequenced on an Illumina apparatus (paired-ended 150 bp reads). The sequencing generated 9.2 million (± 6 million) pairs of reads (**Table S2**).

Sequencing QC and human read removal

To remove low quality reads and the "adaptase" tail characteristic of the xGen kit, raw sequencing reads were processed using fastp version 0.23.1[60] with the following settings: *--trim_front1 2 --trim_tail1 2 --trim_front2 15 --trim_tail2 2 -r -W 4 -M 20 -u 30 -e 20 -l 100*.

The reads of the human host were removed by mapping the cleaned reads against the human genome (GRCh38 version) using bowtie2 version 2.4.1[61] with the *--very-sensitive* option. After this step, four samples had less than 100,000 pairs of reads remaining (H7_F, H10_F, H13_B, CD7_B) and were thus removed from subsequent analysis.

Assembly

The assembly was performed using the cleaned, non-human reads both per individual (using blood and fecal samples together), and with the reads from all the samples of all the individuals altogether (cross-assembly). In both cases, both paired-end and unpaired reads were used, and all the reads were deduplicated prior to the assembly using the dedupe function of bbmap version 38.86[62].

The assembly was then performed using SPAdes version 3.14.0[63] with default parameters, which slightly outperformed metaspades and metaviralspades in number and average size of

contigs. Quality of the assemblies was assessed using QUAST version 5.2.0[64]. Contigs < 2 kb, which correspond to the minimal size of DNA viral genomes, were removed.

Delimitation of OTUs by clustering

Contigs were clustered to delimit OTUs using an approach adapted from Shah et al[34]. First, pairwise alignment of all the contigs was performed using BLAT version 36[65]. The contigs having a total alignment length against themselves > 110% were considered chimeras and removed. For the remaining contigs, clustering was performed at the 95% average nucleotide identity (ANI), corresponding to species boundaries, using scripts described in Shah et al[34].

vOTU detection

Two approaches were combined to detect vOTUs: dedicated tools and homology to virus databases. For the tools, VirSorter2 version 2.2.3[66] was used with the following parameters to increase stringency: *--include-groups dsDNAphage,NCLDV,RNA,ssDNA,lavidaviridae --exclude-lt2gene --min-length 2000 --viral-gene-required --hallmark-required --min-score 0.9 --high-confidence-only*. We included in our viral dataset all the OTUs predicted to be viral. VIBRANT version 1.2.1[67] was also used, and all OTUs predicted as viral were included. CheckV version 0.8.1[28] was also run on all of the OTUs. Only the OTUs with a viral quality above "medium" were included. The comparison between the outputs of these three tools is represented in **Fig. S1**.

For the databases, the OTUs were compared to the COPSAC[34], the GVD[30], the MGV[31], the GPD[32], RefSeq Virus[68] (12/07/2023 release) and the CHVD[33] databases using BLAT version 36[65]. OTUs having > 90% ANI homology to at least one database were considered viral. The comparison between the outputs of the five gut databases is displayed in **Fig. S2**. Finally, the vOTUs of both methods were combined to form a non-redundant list of 17,454 viral vOTUs (**Fig. S3**).

vOTU annotation

The vOTUs were annotated using a modified version of the RimeTOOLS2 Pipeline, from Rime Bioinformatics. Coding sequences (CDS) and tRNAs were predicted using the following tools: prodigal 2.6.3[69] (option -meta), phanotate 1.5.0[70] (default parameters), glimmer 3.02[71] (options long-orfs: -n -t 1.1.15 ; -o 50 -g 110 -t 30), genemarks 1.14[72] (options -m heu_11.mod, -r) and tRNA-scan-SE 2.0.7[73] (option -B). tRNAs were detected first and used to mask the genome sequence, before a 2-tool consensus prediction of CDS using prodigal, phanotate, glimmer, and genemarks. Only CDS called by at least two independent tools were considered, and the longest CDS was prioritized in case of conflict. CDS were subsequently used to query gene and protein databases (CARD 05/2023[74], Resfinder 04/2023[75], VFDB 05/2023[76], Phantome 03/2021, Swissprot 05/2023[77], NCBI Virus 15/2023, Vog 05/2020, Pvog 03/2021[78], Refseq 05/2023[68], DefenseFinder 05/2023[79], and PHROGs 05/2023[80]) using HMMER 3.3.2[81] (E-value < 0.00001, Coverage > 0.7), HHsuite 3.3.2[82] (E-value < 0.00001, Coverage > 0.7, Probability > 90%, Score > 30), and Blast+ 2.9.0[83] (E-value < 0.00001, Identity > 0.7, Coverage

> 0.7). Consensual results with high match scores were kept for the final functional annotation, and prioritized depending on the database of origin (PHROGs > Resfinder, VFDB, DefenseFinder, CARD, Swissprot > Phantome, pVOG, VOG > Refseq).

vOTU classification

To classify the vOTUs, viral proteins (see "vOTU annotation" section) were combined with those of the INPHARED database[84] (02/07/2023 release), and used as input for clustering using vContact2 version 0.9.19[85] using default parameters. Then, graphanalyzer version 1.5.1[86] was used to assign a classification from the network generated by vContact2. A classification was obtained for 2,217 vOTUs (13% of vOTUs).

vOTU lifestyle prediction

The prediction of the lifestyle for the vOTUs was done by searching for integrases in the annotated viral genomes. Only high-quality or complete genomes, as assessed by CheckV, were considered for this analysis. vOTUs classified as Microviridae were also excluded, as their lifestyle cannot be predicted by the presence of integrases[87]. Genes were considered as integrases when either: "integrase" was present in the gene product name, "int" was the gene name, or when both "recombinase" and either "serine" or "tyrosine" are present in the gene product name. vOTUs with at least one integrase were considered as having a temperate lifestyle.

vOTU host prediction

Host prediction for vOTUs was performed using iPHoP version 1.2.0[88] with the associated database (09/2021 release) using default parameters. For both "genome" (host-based tools only) and "genus" (host- and phage-based tools), the best hit for each vOTU was kept. When a vOTU had a hit for both modes, the "genus" prediction was favored. A host was predicted for 13,856 vOTUs (79% of vOTUs).

Non-viral OTUs classification

All OTUs, including the non-viral OTUs, were classified using CAT version 5.2.3[89] using default parameters.

Identification of eukaryotic viruses

All OTUs were compared to the RefSeq Virus database using BLAT (see "vOTU identification" section). The OTUs homologous to RefSeq Virus were hand-curated to removed viruses of bacteria and archaea in order to identify the eukaryotic viruses.

Relative abundances calculation

Cleaned, non-human reads were mapped using bwa-mem2 version 2.2.1[90] against all the OTUs, using default parameters. The resulting SAM file was converted to BAM and sorted by read name using samtools version 1.9[91], before filtering out the low-quality alignments using

msamtools filter version 1.1.3. Alignments > 80 bp with > 95% identity over > 80% sequence length were selected, and only the best alignment (or alignments in the case of multiple alignments with the best score) for each read were kept. The alignments were transformed into counts using msamtools profile, with the *multi=proportional* option so that reads mapping to different OTUs were allocated to the OTUs relatively to their abundances. The coverage and depth of each OTU for each sample was determined using msamtools coverage. OTUs for which sequence coverage was either smaller than 50% of the OTU size or the average sequencing depth was smaller than 1 in a given sample were discarded by setting their count to 0 in this sample. The OTUs present in the negative control samples were set to 0 counts in all the other samples to remove contaminants. Given the disparity in number of viral counts for blood and fecal samples and their separate analysis, rarefaction was performed separately for each. For fecal samples, counts were rarefied at the lowest number of viral counts (267,514 counts). For blood samples, counts were rarefied at 7,653 viral counts (three samples were excluded by this rarefaction). Counts were then normalized by vOTU length and transformed into relative abundances to allow for comparison across vOTUs and samples. This resulted in the main abundance table used for the analysis.

For the analysis of negative control samples and of non-viral OTUs, a similar approach was performed. After the coverage criteria were applied, the entire count table was directly normalized by OTU length and transformed in relative abundances before analysis.

Ecological analysis

The relative abundance table was analysed in tandem with a taxonomy table, containing all the information gathered about each vOTU (length, quality, predicted host, annotation, …) with the R package phyloseq version 1.46.0[92]. The R package vegan version 2.6.4[93] was used for the Adonis2 multivariate analysis.

Estimation of the number of viral particles in samples by spiking

In order to estimate the number of viral particles in the samples, we employed a spiking approach using two phages : a dsDNA phage, SPP1 (host *Bacillus subtilis*) and a ssDNA phage, M13 (host *Escherichia coli*). In fecal samples, a concentration of 10^6 plaque-forming units (PFU) per mL of both SPP1 and M13 was used for all samples. In blood samples, two concentrations were used: 10^6 PFU/mL for both SPP1 and M13 for samples H1 to H5 and CD1 to CD5, and 10^4 PFU/mL for the other samples. The vOTUs corresponding to SPP1 and M13 were identified by homology search against the reference genomes of these phages, using vsearch version 2.18.0[94]. Then, for each sample, the relative abundance of both SPP1 and M13 was calculated using the corresponding concentration spiked in the sample, in order to generate an estimation of the number of viral particles contained in the rest of the sample (contaminant and non-viral OTUs were removed before this step). Then, the values obtained for SPP1 and M13 were averaged. This number was finally normalized by the weight of the fecal sample (0.2 g for all samples) to generate viral particles per g of feces estimates for fecal samples, or

by the volume of blood used (3 mL for all samples) to generate viral particles per mL of blood for plasma samples.

Determination of the origin of the blood vOTUs

In order to determine the origin of the vOTUs, the comparison of the OTUs against gut viral databases (COPSAC, CHVD, GVD, GPD) was used (see "vOTU detection" section). With a threshold of > 90% ANI, blood vOTUs having homology against at least one these databases were considered as having a gut origin. The Oral Virus Database[36] was used in the same manner in order to find blood vOTUs having an oral origin.

Differential analysis

To identify vOTUs responsible for the different blood viral communities in CD patients and healthy individuals, differential analysis was conducted using the Maaslin2 R package[95]. The minimum prevalence was of five samples, and no minimal abundance was set. Normalization was performed by total sum scaling, and the analysis method was LM (both are default parameters). The fixed effects were the disease status (CD/healthy) and the sex. The age, which was statistically lower in the control group (median age: 42 in the CD group and 30 in the healthy group, p=0.0027, one-way ANOVA), could not be added in the model. Only the vOTUs for which q-value < 0.25 and |Log2FC| > 1 were considered significant.

Statistical analysis

All statistical analysis was performed using R version 4.3.2[96]. On the boxplot displayed in the figures, the middle line represents the median value, the bottom and top edge of the box represent respectively the lower and upper quartiles, and the whiskers extends from the edges of the box to the largest or smallest value no further than 1.5 times the inter-quartile range. Pairwise comparisons were performed with the Wilcoxon test.

Acknowledgements

We thank Nicolas Dufour for valuable discussion and his suggestion to include the blood collection tube as a negative control. We thank Marius Bredon for his advice on the differential analysis. We thank Sophie Thenet, Véronique Carriere, Yanis Sbardella and Clara Douadi for valuable discussions. We thank Eugen Pfeifer for critical review of the manuscript. We also want to thank Rio for his contribution to the virome protocol. We are grateful to the INRAE MIGALE bioinformatics facility (MIGALE, INRAE, 2020. Migale bioinformatics Facility, doi: 10.15454/1.5572390655343293E12) for providing computing and storage resources. Finally, for the sequencing, we thank M. Monot, GM Haustant, L. Lemée Biomics Platform, C2RT, Institut Pasteur, Paris, France, supported by France Génomique (ANR-10-INBS-09-09) and IBISA.

Funding

This work was funded by the ANR Primavera (ANR-19-CE18-0028) and the Société Nationale Française de Gastro-Entérologie (SNFGE).

References

1. Olde Loohuis, L.M., Mangul, S., Ori, A.P.S., Jospin, G., Koslicki, D., Yang, H.T., Wu, T., Boks, M.P., Lomen-Hoerth, C., Wiedau-Pazos, M., et al. (2018). Transcriptome analysis in whole blood reveals increased microbial diversity in schizophrenia. Transl Psychiatry *8*, 1–9. https://doi.org/10.1038/s41398-018-0107-9.

2. Panaiotov, S., Filevski, G., Equestre, M., Nikolova, E., and Kalfin, R. (2018). Cultural Isolation and Characteristics of the Blood Microbiome of Healthy Individuals. Advances in Microbiology *8*, 406–421. https://doi.org/10.4236/aim.2018.85027.

3. Li, Q., Wang, C., Tang, C., Zhao, X., He, Q., and Li, J. (2018). Identification and Characterization of Blood and Neutrophil-Associated Microbiomes in Patients with Severe Acute Pancreatitis Using Next-Generation Sequencing. Front. Cell. Infect. Microbiol. *8*. https://doi.org/10.3389/fcimb.2018.00005.

4. Païssé, S., Valle, C., Servant, F., Courtney, M., Burcelin, R., Amar, J., and Lelouvier, B. (2016). Comprehensive description of blood microbiome from healthy donors assessed by 16S targeted metagenomic sequencing. Transfusion *56*, 1138–1147. https://doi.org/10.1111/trf.13477.

5. Whittle, E., Leonard, M.O., and Tonge, D.P. (2019). Multi-Method Characterization of the Human Circulating Microbiome. Front. Microbiol. *9*. https://doi.org/10.3389/fmicb.2018.03266.

6. Tan, C.C.S., Ko, K.K.K., Chen, H., Liu, J., Loh, M., Chia, M., and Nagarajan, N. (2023). No evidence for a common blood microbiome based on a population study of 9,770 healthy humans. Nat Microbiol *8*, 973–985. https://doi.org/10.1038/s41564-023-01350-w.

7. Cebriá-Mendoza, M., Bracho, M.A., Arbona, C., Larrea, L., Díaz, W., Sanjuán, R., and Cuevas, J.M. (2021). Exploring the Diversity of the Human Blood Virome. Viruses *13*, 2322. https://doi.org/10.3390/v13112322.

8. Furuta, R.A., Sakamoto, H., Kuroishi, A., Yasiui, K., Matsukura, H., and Hirayama, F. (2015). Metagenomic profiling of the viromes of plasma collected from blood donors with elevated serum alanine aminotransferase levels. Transfusion *55*, 1889–1899. https://doi.org/10.1111/trf.13057.

9. Stout, M.J., Brar, A.K., Herter, B.N., Rankin, A., and Wylie, K.M. (2023). The plasma virome in longitudinal samples from pregnant patients. Front. Cell. Infect. Microbiol. *13*. https://doi.org/10.3389/fcimb.2023.1061230.

10. Thijssen, M., Khamisipour, G., Maleki, M., Devos, T., Li, G., Van Ranst, M., Matthijnssens, J., and Pourkarim, M.R. (2023). Characterization of the Human Blood Virome in Iranian Multiple Transfused Patients. Viruses *15*, 1425. https://doi.org/10.3390/v15071425.

11. Yang, K., Niu, J., Zuo, T., Sun, Y., Xu, Z., Tang, W., Liu, Q., Zhang, J., Ng, E.K.W., Wong, S.K.H., et al. (2021). Alterations in the Gut Virome in Obesity and Type 2 Diabetes Mellitus. Gastroenterology *161*, 1257-1269.e13. https://doi.org/10.1053/j.gastro.2021.06.056.

12. Jiang, L., Lang, S., Duan, Y., Zhang, X., Gao, B., Chopyk, J., Schwanemann, L.K., Ventura-Cots, M., Bataller, R., Bosques-Padilla, F., et al. (2020). Intestinal Virome in Patients With Alcoholic Hepatitis. Hepatology *72*, 2182. https://doi.org/10.1002/hep.31459.

13. Nakatsu, G., Zhou, H., Wu, W.K.K., Wong, S.H., Coker, O.O., Dai, Z., Li, X., Szeto, C.-H., Sugimura, N., Lam, T.Y.-T., et al. (2018). Alterations in Enteric Virome Are Associated With Colorectal Cancer

and Survival Outcomes. Gastroenterology *155*, 529-541.e5. https://doi.org/10.1053/j.gastro.2018.04.018.

14. Mirzaei, M.K., Khan, M.A.A., Ghosh, P., Taranu, Z.E., Taguer, M., Ru, J., Chowdhury, R., Kabir, M.M., Deng, L., Mondal, D., et al. (2020). Bacteriophages Isolated from Stunted Children Can Regulate Gut Bacterial Communities in an Age-Specific Manner. Cell Host & Microbe *27*, 199-212.e5. https://doi.org/10.1016/j.chom.2020.01.004.

15. Bichet, M.C., Chin, W.H., Richards, W., Lin, Y.-W., Avellaneda-Franco, L., Hernandez, C.A., Oddo, A., Chernyavskiy, O., Hilsenstein, V., Neild, A., et al. (2021). Bacteriophage uptake by mammalian cell layers represents a potential sink that may impact phage therapy. iScience *24*, 102287. https://doi.org/10.1016/j.isci.2021.102287.

16. Nguyen, S., Baker, K., Padman, B.S., Patwa, R., Dunstan, R.A., Weston, T.A., Schlosser, K., Bailey, B., Lithgow, T., Lazarou, M., et al. (2017). Bacteriophage Transcytosis Provides a Mechanism To Cross Epithelial Cell Layers. mBio *8*, 10.1128/mbio.01874-17. https://doi.org/10.1128/mbio.01874-17.

17. Haddock, N.L., Barkal, L.J., Ram-Mohan, N., Kaber, G., Chiu, C.Y., Bhatt, A.S., Yang, S., and Bollyky, P.L. (2023). Phage diversity in cell-free DNA identifies bacterial pathogens in human sepsis cases. Nat Microbiol *8*, 1495–1507. https://doi.org/10.1038/s41564-023-01406-x.

18. Moustafa, A., Xie, C., Kirkness, E., Biggs, W., Wong, E., Turpaz, Y., Bloom, K., Delwart, E., Nelson, K.E., Venter, J.C., et al. (2017). The blood DNA virome in 8,000 humans. PLOS Pathogens *13*, e1006292. https://doi.org/10.1371/journal.ppat.1006292.

19. Roda, G., Chien Ng, S., Kotze, P.G., Argollo, M., Panaccione, R., Spinelli, A., Kaser, A., Peyrin-Biroulet, L., and Danese, S. (2020). Crohn's disease. Nat Rev Dis Primers *6*, 1–19. https://doi.org/10.1038/s41572-020-0156-2.

20. Sokol, H., Pigneur, B., Watterlot, L., Lakhdari, O., Bermúdez-Humarán, L.G., Gratadoux, J.-J., Blugeon, S., Bridonneau, C., Furet, J.-P., Corthier, G., et al. (2008). Faecalibacterium prausnitzii is an anti-inflammatory commensal bacterium identified by gut microbiota analysis of Crohn disease patients. Proc Natl Acad Sci U S A *105*, 16731–16736. https://doi.org/10.1073/pnas.0804812105.

21. Pascal, V., Pozuelo, M., Borruel, N., Casellas, F., Campos, D., Santiago, A., Martinez, X., Varela, E., Sarrabayrouse, G., Machiels, K., et al. (2017). A microbial signature for Crohn's disease. Gut *66*, 813–822. https://doi.org/10.1136/gutjnl-2016-313235.

22. Manichanh, C., Rigottier-Gois, L., Bonnaud, E., Gloux, K., Pelletier, E., Frangeul, L., Nalin, R., Jarrin, C., Chardon, P., Marteau, P., et al. (2006). Reduced diversity of faecal microbiota in Crohn's disease revealed by a metagenomic approach. Gut *55*, 205–211. https://doi.org/10.1136/gut.2005.073817.

23. Norman, J.M., Handley, S.A., Baldridge, M.T., Droit, L., Liu, C.Y., Keller, B.C., Kambal, A., Monaco, C.L., Zhao, G., Fleshner, P., et al. (2015). Disease-Specific Alterations in the Enteric Virome in Inflammatory Bowel Disease. Cell *160*, 447–460. https://doi.org/10.1016/j.cell.2015.01.002.

24. Clooney, A.G., Sutton, T.D.S., Shkoporov, A.N., Holohan, R.K., Daly, K.M., O'Regan, O., Ryan, F.J., Draper, L.A., Plevy, S.E., Ross, R.P., et al. (2019). Whole-Virome Analysis Sheds Light on Viral Dark Matter in Inflammatory Bowel Disease. Cell Host Microbe *26*, 764-778.e5. https://doi.org/10.1016/j.chom.2019.10.009.

25. Zuo, T., Lu, X.-J., Zhang, Y., Cheung, C.P., Lam, S., Zhang, F., Tang, W., Ching, J.Y.L., Zhao, R., Chan, P.K.S., et al. (2019). Gut mucosal virome alterations in ulcerative colitis. Gut *68*, 1169–1179. https://doi.org/10.1136/gutjnl-2018-318131.

26. Stockdale, S.R., Shkoporov, A.N., Khokhlova, E.V., Daly, K.M., McDonnell, S.A., O' Regan, O., Nolan, J.A., Sutton, T.D.S., Clooney, A.G., Ryan, F.J., et al. (2023). Interpersonal variability of the human gut virome confounds disease signal detection in IBD. Commun Biol *6*, 1–10. https://doi.org/10.1038/s42003-023-04592-w.

27. Castillo, D.J., Rifkin, R.F., Cowan, D.A., and Potgieter, M. (2019). The Healthy Human Blood Microbiome: Fact or Fiction? Front. Cell. Infect. Microbiol. *9*. https://doi.org/10.3389/fcimb.2019.00148.

28. Nayfach, S., Camargo, A.P., Schulz, F., Eloe-Fadrosh, E., Roux, S., and Kyrpides, N.C. (2021). CheckV assesses the quality and completeness of metagenome-assembled viral genomes. Nat Biotechnol *39*, 578–585. https://doi.org/10.1038/s41587-020-00774-7.

29. Wiest, R., and Rath, H.C. (2003). Bacterial translocation in the gut. Best Practice & Research Clinical Gastroenterology *17*, 397–425. https://doi.org/10.1016/S1521-6918(03)00024-6.

30. Gregory, A.C., Zablocki, O., Zayed, A.A., Howell, A., Bolduc, B., and Sullivan, M.B. (2020). The Gut Virome Database Reveals Age-Dependent Patterns of Virome Diversity in the Human Gut. Cell Host & Microbe *28*, 724-740.e8. https://doi.org/10.1016/j.chom.2020.08.003.

31. Nayfach, S., Páez-Espino, D., Call, L., Low, S.J., Sberro, H., Ivanova, N.N., Proal, A.D., Fischbach, M.A., Bhatt, A.S., Hugenholtz, P., et al. (2021). Metagenomic compendium of 189,680 DNA viruses from the human gut microbiome. Nat Microbiol *6*, 960–970. https://doi.org/10.1038/s41564-021-00928-6.

32. Camarillo-Guerrero, L.F., Almeida, A., Rangel-Pineros, G., Finn, R.D., and Lawley, T.D. (2021). Massive expansion of human gut bacteriophage diversity. Cell *184*, 1098-1109.e9. https://doi.org/10.1016/j.cell.2021.01.029.

33. Tisza, M.J., and Buck, C.B. (2021). A catalog of tens of thousands of viruses from human metagenomes reveals hidden associations with chronic diseases. Proceedings of the National Academy of Sciences *118*, e2023202118. https://doi.org/10.1073/pnas.2023202118.

34. Shah, S.A., Deng, L., Thorsen, J., Pedersen, A.G., Dion, M.B., Castro-Mejía, J.L., Silins, R., Romme, F.O., Sausset, R., Jessen, L.E., et al. (2023). Expanding known viral diversity in the healthy infant gut. Nat Microbiol *8*, 986–998. https://doi.org/10.1038/s41564-023-01345-7.

35. Cho, I., and Blaser, M.J. (2012). The human microbiome: at the interface of health and disease. Nat Rev Genet *13*, 260–270. https://doi.org/10.1038/nrg3182.

36. Li, S., Guo, R., Zhang, Y., Li, P., Chen, F., Wang, X., Li, J., Jie, Z., Lv, Q., Jin, H., et al. (2022). A catalog of 48,425 nonredundant viruses from oral metagenomes expands the horizon of the human oral virome. iScience *25*, 104418. https://doi.org/10.1016/j.isci.2022.104418.

37. Imhann, F., Vila, A.V., Bonder, M.J., Fu, J., Gevers, D., Visschedijk, M.C., Spekhorst, L.M., Alberts, R., Franke, L., Dullemen, H.M. van, et al. (2018). Interplay of host genetics and gut microbiota underlying the onset and clinical presentation of inflammatory bowel disease. Gut *67*, 108–119. https://doi.org/10.1136/gutjnl-2016-312135.

38. Withatanung, P., Janesomboon, S., Vanaporn, M., Muangsombut, V., Charoensudjai, S., Baker, D.J., Wuthiekanun, V., Galyov, E.E., Clokie, M.R.J., Gundogdu, O., et al. (2024). Induced Burkholderia prophages detected from the hemoculture: a biomarker for Burkholderia pseudomallei infection. Front. Microbiol. *15*. https://doi.org/10.3389/fmicb.2024.1361121.

39. Shkoporov, A.N., Turkington, C.J., and Hill, C. (2022). Mutualistic interplay between bacteriophages and bacteria in the human gut. Nat Rev Microbiol *20*, 737–749. https://doi.org/10.1038/s41579-022-00755-4.

40. Shah, N.B., Nigwekar, S.U., Kalim, S., Lelouvier, B., Servant, F., Dalal, M., Krinsky, S., Fasano, A., Tolkoff-Rubin, N., and Allegretti, A.S. (2021). The Gut and Blood Microbiome in IgA Nephropathy and Healthy Controls. Kidney360 *2*, 1261–1274. https://doi.org/10.34067/KID.0000132021.

41. Shkoporov, A.N., and Hill, C. (2019). Bacteriophages of the Human Gut: The “Known Unknown” of the Microbiome. Cell Host & Microbe *25*, 195–209. https://doi.org/10.1016/j.chom.2019.01.017.

42. Moses, S., Vagima, Y., Tidhar, A., Aftalion, M., Mamroud, E., Rotem, S., and Steinberger-Levy, I. (2021). Characterization of Yersinia pestis Phage Lytic Activity in Human Whole Blood for the Selection of Efficient Therapeutic Phages. Viruses *13*, 89. https://doi.org/10.3390/v13010089.

43. Mutti, M., Moreno, D.S., Restrepo-Córdoba, M., Visram, Z., Resch, G., and Corsini, L. (2023). Phage activity against Staphylococcus aureus is impaired in plasma and synovial fluid. Sci Rep *13*, 18204. https://doi.org/10.1038/s41598-023-45405-8.

44. Sweere, J.M., Van Belleghem, J.D., Ishak, H., Bach, M.S., Popescu, M., Sunkari, V., Kaber, G., Manasherob, R., Suh, G.A., Cao, X., et al. (2019). Bacteriophage trigger antiviral immunity and prevent clearance of bacterial infection. Science *363*, eaat9691. https://doi.org/10.1126/science.aat9691.

45. Leal Rodríguez, C., Shah, S.A., Rasmussen, M.A., Thorsen, J., Boulund, U., Pedersen, C.-E.T., Castro-Mejía, J.L., Poulsen, C.E., Poulsen, C.S., Deng, L., et al. (2024). The infant gut virome is associated with preschool asthma risk independently of bacteria. Nat Med *30*, 138–148. https://doi.org/10.1038/s41591-023-02685-x.

46. Fluckiger, A., Daillère, R., Sassi, M., Sixt, B.S., Liu, P., Loos, F., Richard, C., Rabu, C., Alou, M.T., Goubet, A.-G., et al. (2020). Cross-reactivity between tumor MHC class I-restricted antigens and an enterococcal bacteriophage. Science *369*, 936–942. https://doi.org/10.1126/science.aax0701.

47. Cao, Z., Fan, D., Sun, Y., Huang, Z., Li, Y., Su, R., Zhang, F., Li, Q., Yang, H., Zhang, F., et al. (2024). The gut ileal mucosal virome is disturbed in patients with Crohn’s disease and exacerbates intestinal inflammation in mice. Nat Commun *15*, 1638. https://doi.org/10.1038/s41467-024-45794-y.

48. Popgeorgiev, N., Krupovic, M., Hiblot, J., Fancello, L., Monteil-Bouchard, S., and Desnues, C. (2024). A New Inovirus from the Human Blood Encodes Proteins with Nuclear Subcellular Localization. Viruses *16*, 475. https://doi.org/10.3390/v16030475.

49. Ingle, H., Lee, S., Ai, T., Orvedahl, A., Rodgers, R., Zhao, G., Sullender, M., Peterson, S.T., Locke, M., Liu, T.-C., et al. (2019). Viral complementation of immunodeficiency confers protection against enteric pathogens via IFN-λ. Nat Microbiol *4*, 1120–1128. https://doi.org/10.1038/s41564-019-0416-7.

50. Dallari, S., Heaney, T., Rosas-Villegas, A., Neil, J.A., Wong, S.-Y., Brown, J.J., Urbanek, K., Herrmann, C., Depledge, D.P., Dermody, T.S., et al. (2021). Enteric viruses evoke broad host immune responses resembling those elicited by the bacterial microbiome. Cell Host & Microbe *29*, 1014-1029.e8. https://doi.org/10.1016/j.chom.2021.03.015.

51. Liu, L., Gong, T., Tao, W., Lin, B., Li, C., Zheng, X., Zhu, S., Jiang, W., and Zhou, R. (2019). Commensal viruses maintain intestinal intraepithelial lymphocytes via noncanonical RIG-I signaling. Nat Immunol *20*, 1681–1691. https://doi.org/10.1038/s41590-019-0513-z.

52. Dąbrowska, K. (2019). Phage therapy: What factors shape phage pharmacokinetics and bioavailability? Systematic and critical review. Medicinal Research Reviews *39*, 2000–2025. https://doi.org/10.1002/med.21572.

53. Shalon, D., Culver, R.N., Grembi, J.A., Folz, J., Treit, P.V., Shi, H., Rosenberger, F.A., Dethlefsen, L., Meng, X., Yaffe, E., et al. (2023). Profiling the human intestinal environment under physiological conditions. Nature *617*, 581–591. https://doi.org/10.1038/s41586-023-05989-7.

54. Vuik, F., Dicksved, J., Lam, S., Fuhler, G., van der Laan, L., van de Winkel, A., Konstantinov, S., Spaander, M., Peppelenbosch, M., Engstrand, L., et al. (2019). Composition of the mucosa-associated microbiota along the entire gastrointestinal tract of human individuals. United European Gastroenterology Journal *7*, 897–907. https://doi.org/10.1177/2050640619852255.

55. Camilleri, M. (2021). Human Intestinal Barrier: Effects of Stressors, Diet, Prebiotics, and Probiotics. Clinical and Translational Gastroenterology *12*, e00308. https://doi.org/10.14309/ctg.0000000000000308.

56. Flowers, L., and Grice, E.A. (2020). The Skin Microbiota: Balancing Risk and Reward. Cell Host & Microbe *28*, 190–200. https://doi.org/10.1016/j.chom.2020.06.017.

57. Willner, D., Furlan, M., Haynes, M., Schmieder, R., Angly, F.E., Silva, J., Tammadoni, S., Nosrat, B., Conrad, D., and Rohwer, F. (2009). Metagenomic Analysis of Respiratory Tract DNA Viral Communities in Cystic Fibrosis and Non-Cystic Fibrosis Individuals. PLOS ONE *4*, e7370. https://doi.org/10.1371/journal.pone.0007370.

58. Billaud, M., Lamy-Besnier, Q., Lossouarn, J., Moncaut, E., Dion, M.B., Moineau, S., Traoré, F., Le Chatelier, E., Denis, C., Estelle, J., et al. (2021). Analysis of viromes and microbiomes from pig fecal samples reveals that phages and prophages rarely carry antibiotic resistance genes. ISME COMMUN. *1*, 1–10. https://doi.org/10.1038/s43705-021-00054-8.

59. Trubl, G., Roux, S., Solonenko, N., Li, Y.-F., Bolduc, B., Rodríguez-Ramos, J., Eloe-Fadrosh, E.A., Rich, V.I., and Sullivan, M.B. (2019). Towards optimized viral metagenomes for double-stranded and single-stranded DNA viruses from challenging soils. PeerJ *7*, e7265. https://doi.org/10.7717/peerj.7265.

60. Chen, S., Zhou, Y., Chen, Y., and Gu, J. (2018). fastp: an ultra-fast all-in-one FASTQ preprocessor. Bioinformatics *34*, i884–i890. https://doi.org/10.1093/bioinformatics/bty560.

61. Langmead, B., and Salzberg, S.L. (2012). Fast gapped-read alignment with Bowtie 2. Nat Methods *9*, 357–359. https://doi.org/10.1038/nmeth.1923.

62. Bushnell, B. (2014). BBMap: A Fast, Accurate, Splice-Aware Aligner (Lawrence Berkeley National Lab. (LBNL), Berkeley, CA (United States)).

63. Prjibelski, A., Antipov, D., Meleshko, D., Lapidus, A., and Korobeynikov, A. (2020). Using SPAdes De Novo Assembler. Current Protocols in Bioinformatics *70*, e102. https://doi.org/10.1002/cpbi.102.

64. Gurevich, A., Saveliev, V., Vyahhi, N., and Tesler, G. (2013). QUAST: quality assessment tool for genome assemblies. Bioinformatics *29*, 1072–1075. https://doi.org/10.1093/bioinformatics/btt086.

65. Kent, W.J. (2002). BLAT—The BLAST-Like Alignment Tool. Genome Res *12*, 656–664. https://doi.org/10.1101/gr.229202.

66. Guo, J., Bolduc, B., Zayed, A.A., Varsani, A., Dominguez-Huerta, G., Delmont, T.O., Pratama, A.A., Gazitúa, M.C., Vik, D., Sullivan, M.B., et al. (2021). VirSorter2: a multi-classifier, expert-guided approach to detect diverse DNA and RNA viruses. Microbiome *9*, 37. https://doi.org/10.1186/s40168-020-00990-y.

67. Kieft, K., Zhou, Z., and Anantharaman, K. (2020). VIBRANT: automated recovery, annotation and curation of microbial viruses, and evaluation of viral community function from genomic sequences. Microbiome *8*, 90. https://doi.org/10.1186/s40168-020-00867-0.

68. O'Leary, N.A., Wright, M.W., Brister, J.R., Ciufo, S., Haddad, D., McVeigh, R., Rajput, B., Robbertse, B., Smith-White, B., Ako-Adjei, D., et al. (2016). Reference sequence (RefSeq) database at NCBI: current status, taxonomic expansion, and functional annotation. Nucleic Acids Res *44*, D733-745. https://doi.org/10.1093/nar/gkv1189.

69. Hyatt, D., Chen, G.-L., LoCascio, P.F., Land, M.L., Larimer, F.W., and Hauser, L.J. (2010). Prodigal: prokaryotic gene recognition and translation initiation site identification. BMC Bioinformatics *11*, 119. https://doi.org/10.1186/1471-2105-11-119.

70. McNair, K., Zhou, C., Dinsdale, E.A., Souza, B., and Edwards, R.A. (2019). PHANOTATE: a novel approach to gene identification in phage genomes. Bioinformatics *35*, 4537–4542. https://doi.org/10.1093/bioinformatics/btz265.

71. Delcher, A.L., Bratke, K.A., Powers, E.C., and Salzberg, S.L. (2007). Identifying bacterial genes and endosymbiont DNA with Glimmer. Bioinformatics *23*, 673–679. https://doi.org/10.1093/bioinformatics/btm009.

72. Besemer, J., Lomsadze, A., and Borodovsky, M. (2001). GeneMarkS: a self-training method for prediction of gene starts in microbial genomes. Implications for finding sequence motifs in regulatory regions. Nucleic Acids Res *29*, 2607–2618. https://doi.org/10.1093/nar/29.12.2607.

73. Lowe, T.M., and Chan, P.P. (2016). tRNAscan-SE On-line: integrating search and context for analysis of transfer RNA genes. Nucleic Acids Res *44*, W54-57. https://doi.org/10.1093/nar/gkw413.

74. Alcock, B.P., Huynh, W., Chalil, R., Smith, K.W., Raphenya, A.R., Wlodarski, M.A., Edalatmand, A., Petkau, A., Syed, S.A., Tsang, K.K., et al. (2023). CARD 2023: expanded curation, support for machine learning, and resistome prediction at the Comprehensive Antibiotic Resistance Database. Nucleic Acids Res *51*, D690–D699. https://doi.org/10.1093/nar/gkac920.

75. Florensa, A.F., Kaas, R.S., Clausen, P.T.L.C., Aytan-Aktug, D., and Aarestrup, F.M. (2022). ResFinder - an open online resource for identification of antimicrobial resistance genes in next-generation

sequencing data and prediction of phenotypes from genotypes. Microb Genom *8*, 000748. https://doi.org/10.1099/mgen.0.000748.

76. Liu, B., Zheng, D., Jin, Q., Chen, L., and Yang, J. (2019). VFDB 2019: a comparative pathogenomic platform with an interactive web interface. Nucleic Acids Res *47*, D687–D692. https://doi.org/10.1093/nar/gky1080.

77. Boutet, E., Lieberherr, D., Tognolli, M., Schneider, M., and Bairoch, A. (2007). UniProtKB/Swiss-Prot. Methods Mol Biol *406*, 89–112. https://doi.org/10.1007/978-1-59745-535-0_4.

78. Grazziotin, A.L., Koonin, E.V., and Kristensen, D.M. (2017). Prokaryotic Virus Orthologous Groups (pVOGs): a resource for comparative genomics and protein family annotation. Nucleic Acids Res *45*, D491–D498. https://doi.org/10.1093/nar/gkw975.

79. Tesson, F., Hervé, A., Mordret, E., Touchon, M., d'Humières, C., Cury, J., and Bernheim, A. (2022). Systematic and quantitative view of the antiviral arsenal of prokaryotes. Nat Commun *13*, 2561. https://doi.org/10.1038/s41467-022-30269-9.

80. Terzian, P., Olo Ndela, E., Galiez, C., Lossouarn, J., Pérez Bucio, R.E., Mom, R., Toussaint, A., Petit, M.-A., and Enault, F. (2021). PHROG: families of prokaryotic virus proteins clustered using remote homology. NAR Genom Bioinform *3*, lqab067. https://doi.org/10.1093/nargab/lqab067.

81. Mistry, J., Finn, R.D., Eddy, S.R., Bateman, A., and Punta, M. (2013). Challenges in homology search: HMMER3 and convergent evolution of coiled-coil regions. Nucleic Acids Res *41*, e121. https://doi.org/10.1093/nar/gkt263.

82. Steinegger, M., Meier, M., Mirdita, M., Vöhringer, H., Haunsberger, S.J., and Söding, J. (2019). HH-suite3 for fast remote homology detection and deep protein annotation. BMC Bioinformatics *20*, 473. https://doi.org/10.1186/s12859-019-3019-7.

83. Camacho, C., Coulouris, G., Avagyan, V., Ma, N., Papadopoulos, J., Bealer, K., and Madden, T.L. (2009). BLAST+: architecture and applications. BMC Bioinformatics *10*, 421. https://doi.org/10.1186/1471-2105-10-421.

84. Cook, R., Brown, N., Redgwell, T., Rihtman, B., Barnes, M., Clokie, M., Stekel, D.J., Hobman, J., Jones, M.A., and Millard, A. (2021). INfrastructure for a PHAge REference Database: Identification of Large-Scale Biases in the Current Collection of Cultured Phage Genomes. PHAGE *2*, 214–223. https://doi.org/10.1089/phage.2021.0007.

85. Bin Jang, H., Bolduc, B., Zablocki, O., Kuhn, J.H., Roux, S., Adriaenssens, E.M., Brister, J.R., Kropinski, A.M., Krupovic, M., Lavigne, R., et al. (2019). Taxonomic assignment of uncultivated prokaryotic virus genomes is enabled by gene-sharing networks. Nat Biotechnol *37*, 632–639. https://doi.org/10.1038/s41587-019-0100-8.

86. Pandolfo, M., Telatin, A., Lazzari, G., Adriaenssens, E.M., and Vitulo, N. (2022). MetaPhage: an Automated Pipeline for Analyzing, Annotating, and Classifying Bacteriophages in Metagenomics Sequencing Data. mSystems *7*, e00741-22. https://doi.org/10.1128/msystems.00741-22.

87. Krupovic, M., and Forterre, P. (2011). Microviridae Goes Temperate: Microvirus-Related Proviruses Reside in the Genomes of Bacteroidetes. PLOS ONE *6*, e19893. https://doi.org/10.1371/journal.pone.0019893.

88. Roux, S., Camargo, A.P., Coutinho, F.H., Dabdoub, S.M., Dutilh, B.E., Nayfach, S., and Tritt, A. (2023). iPHoP: An integrated machine learning framework to maximize host prediction for metagenome-derived viruses of archaea and bacteria. PLOS Biology *21*, e3002083. https://doi.org/10.1371/journal.pbio.3002083.

89. von Meijenfeldt, F.A.B., Arkhipova, K., Cambuy, D.D., Coutinho, F.H., and Dutilh, B.E. (2019). Robust taxonomic classification of uncharted microbial sequences and bins with CAT and BAT. Genome Biology *20*, 217. https://doi.org/10.1186/s13059-019-1817-x.

90. Vasimuddin, Md., Misra, S., Li, H., and Aluru, S. (2019). Efficient Architecture-Aware Acceleration of BWA-MEM for Multicore Systems. In 2019 IEEE International Parallel and Distributed Processing Symposium (IPDPS), pp. 314–324. https://doi.org/10.1109/IPDPS.2019.00041.

91. Li, H., Handsaker, B., Wysoker, A., Fennell, T., Ruan, J., Homer, N., Marth, G., Abecasis, G., Durbin, R., and 1000 Genome Project Data Processing Subgroup (2009). The Sequence Alignment/Map format and SAMtools. Bioinformatics *25*, 2078–2079. https://doi.org/10.1093/bioinformatics/btp352.

92. McMurdie, P.J., and Holmes, S. (2013). phyloseq: An R Package for Reproducible Interactive Analysis and Graphics of Microbiome Census Data. PLOS ONE *8*, e61217. https://doi.org/10.1371/journal.pone.0061217.

93. Oksanen, J., Simpson, G.L., Blanchet, F.G., Kindt, R., Legendre, P., Minchin, P.R., O'Hara, R.B., Solymos, P., Stevens, M.H.H., Szoecs, E., et al. (2022). vegan: Community Ecology Package. Version 2.6-4.

94. Rognes, T., Flouri, T., Nichols, B., Quince, C., and Mahé, F. (2016). VSEARCH: a versatile open source tool for metagenomics. PeerJ *4*, e2584. https://doi.org/10.7717/peerj.2584.

95. Mallick, H., Rahnavard, A., McIver, L.J., Ma, S., Zhang, Y., Nguyen, L.H., Tickle, T.L., Weingart, G., Ren, B., Schwager, E.H., et al. (2021). Multivariable association discovery in population-scale meta-omics studies. PLOS Computational Biology *17*, e1009442. https://doi.org/10.1371/journal.pcbi.1009442.

96. R: The R Project for Statistical Computing https://www.r-project.org/.

Supplementary Figures

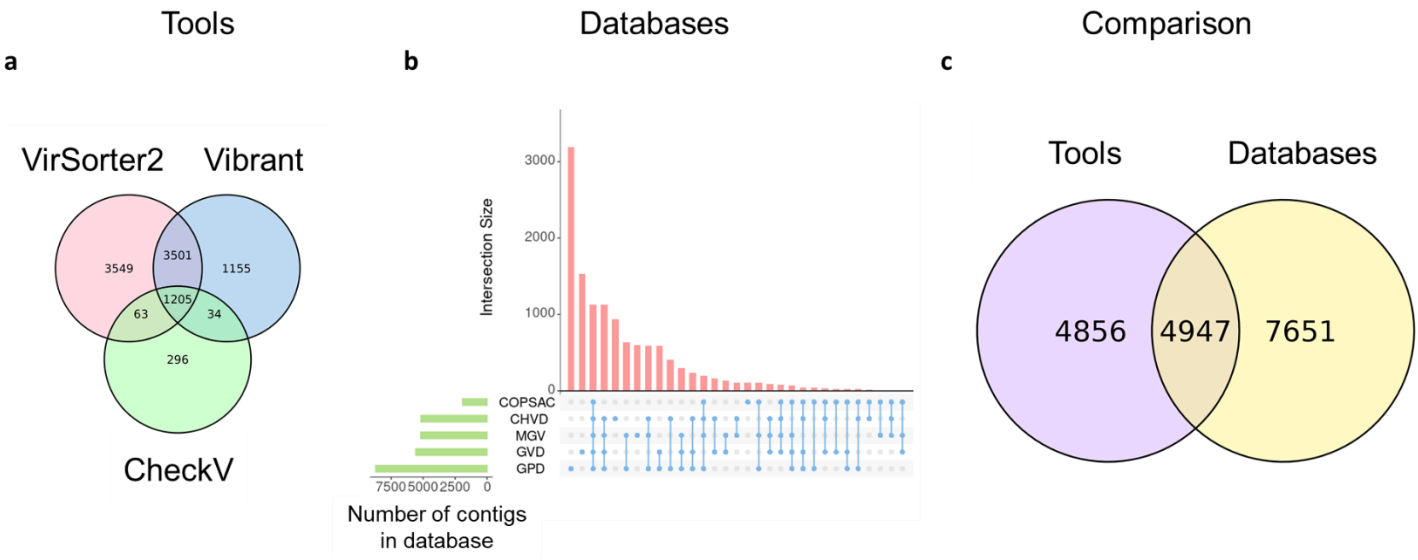

Figure S1: Detection of vOTUs.
a. Venn diagram of the OTUs detected as viral by VirSorter2, VIBRANT and CheckV. **b.** Upset plot of the OTUs detected as viral through homology with five different gut virus databases. **c.** Venn diagram of the OTUs detected as viral by the tools (left) and the databases (right).

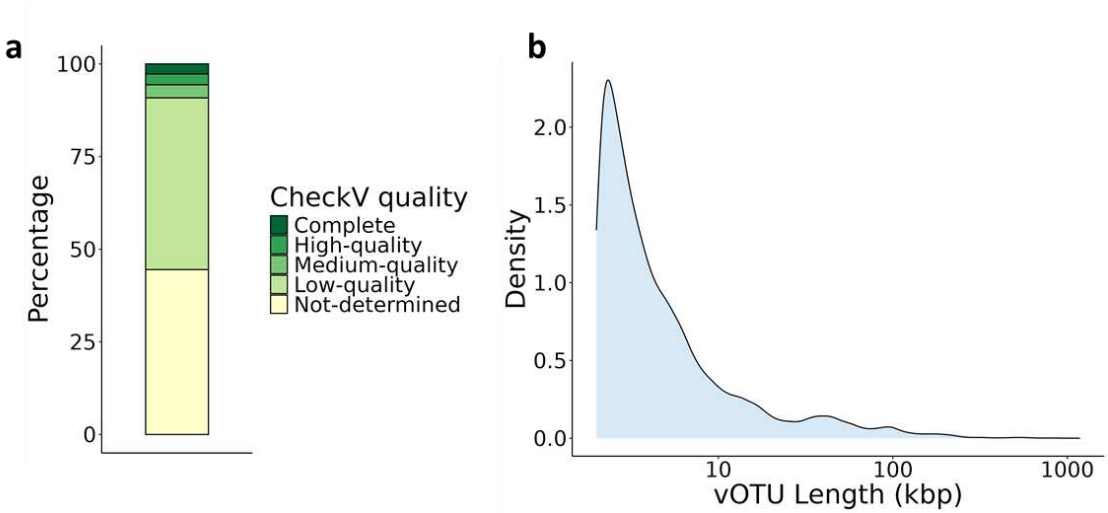

Figure S2: Characteristics of vOTUs.
a. Quality of the vOTUs as determined by CheckV. **b.** Distribution of the length of the vOTUs.

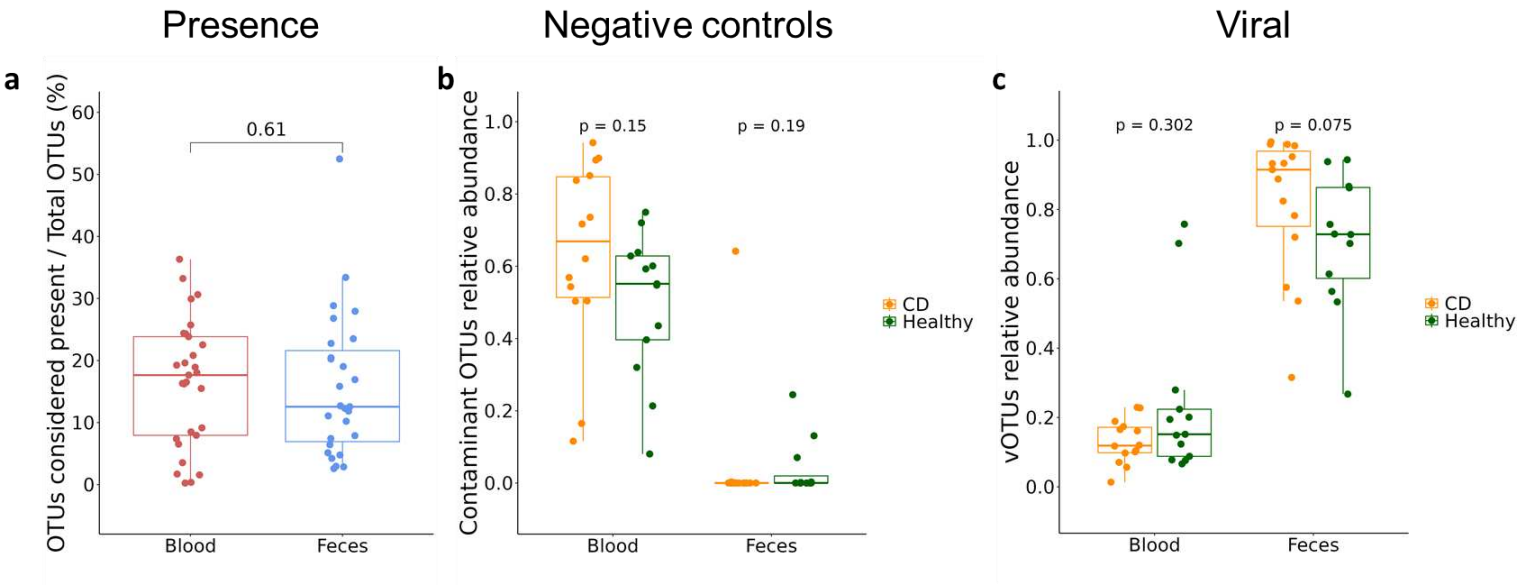

Figure S3: Effects of the different filters used to select non-contaminant vOTUs.
a. Proportion of OTUs that are considered "present" (depth > 1 and coverage > 50%, Methods) per sample, separated by sample type. **b.** Total relative abundance of OTUs that are considered contaminant (i.e. present in negative control samples) per sample, separated by sample type and disease status (orange = CD patients, green = healthy individuals). **c.** After removal of contaminant OTUs (panel b), relative abundance of the OTUs that are considered viral, separated by sample type and disease status (orange = CD patients, green = healthy individuals).

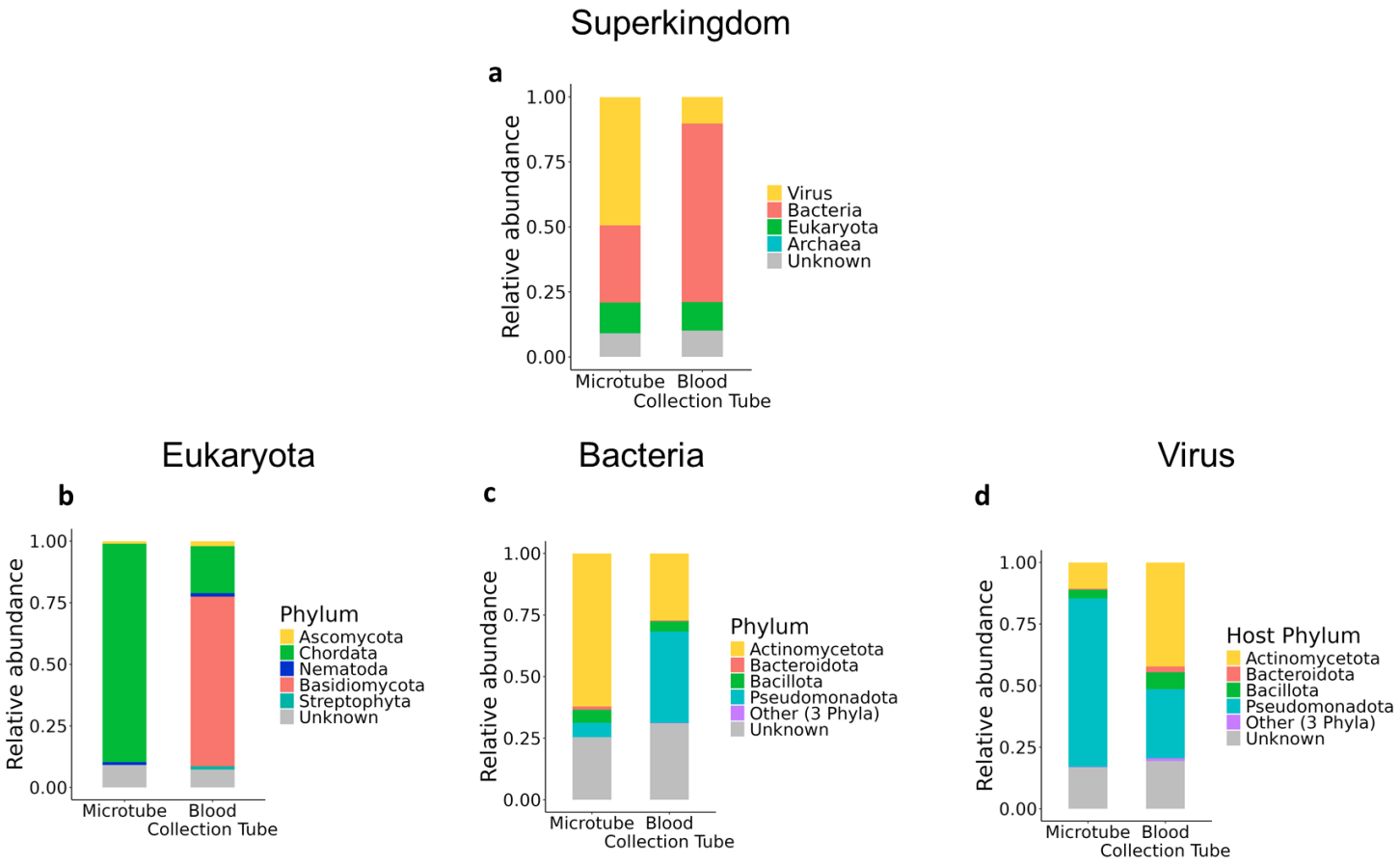

Figure S4: Composition of the negative controls.

a. Composition of both negative control samples, at the superkingdom level. **b.** Composition of the Eukaryota fraction of both negative control samples, at the phylum level. **c.** Composition of the Bacteria fraction of both negative control samples, at the phylum level. **d.** Composition of the Viral fraction of both negative control samples, classed by the predicted host phylum level.

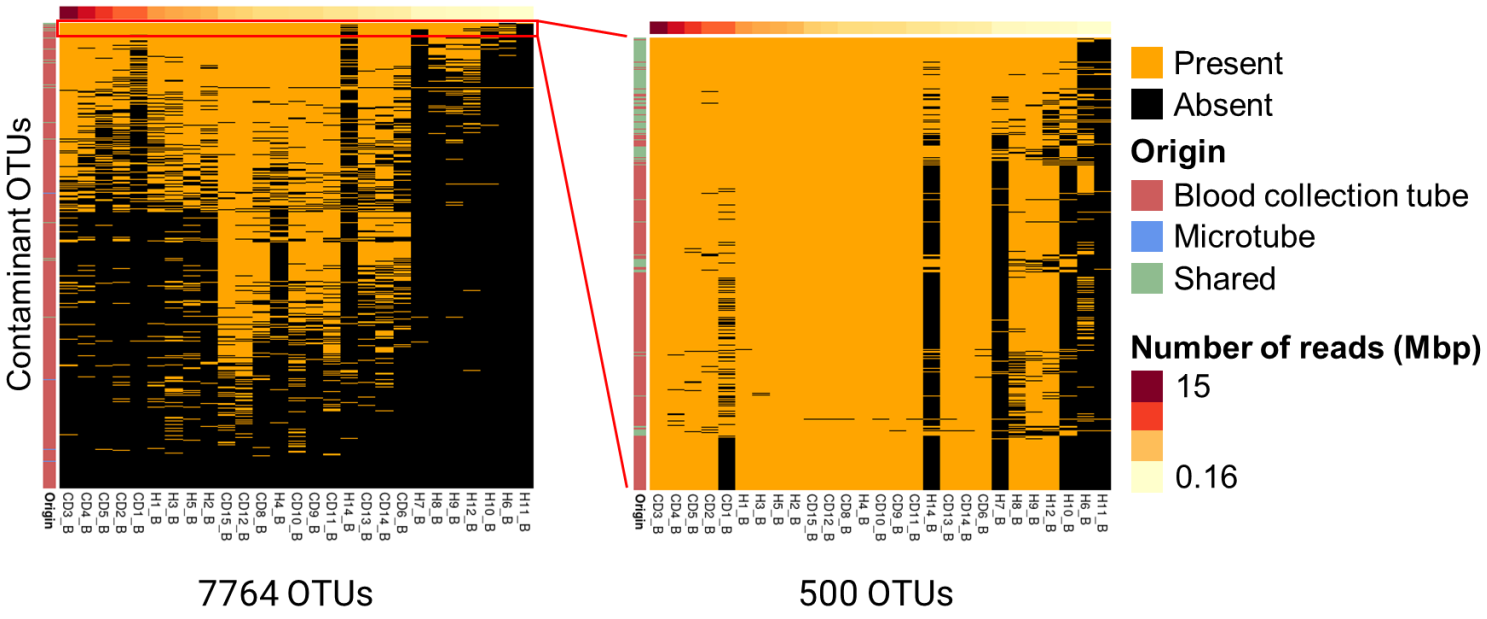

Figure S5: Contamination across samples.
Presence/absence heatmap of the contaminant OTUs (present in negative control samples) across the blood samples. The OTUs are organised top to bottom by decreasing sharedness, and the samples are organised left to right by decreasing number of non-human, cleaned reads. A zoom on the 500 most shared OTUs is displayed on the right panel. The origin (i.e. the sample(s) in which the OTU was found to be present) of each vOTU is displayed on the left of the heatmap.

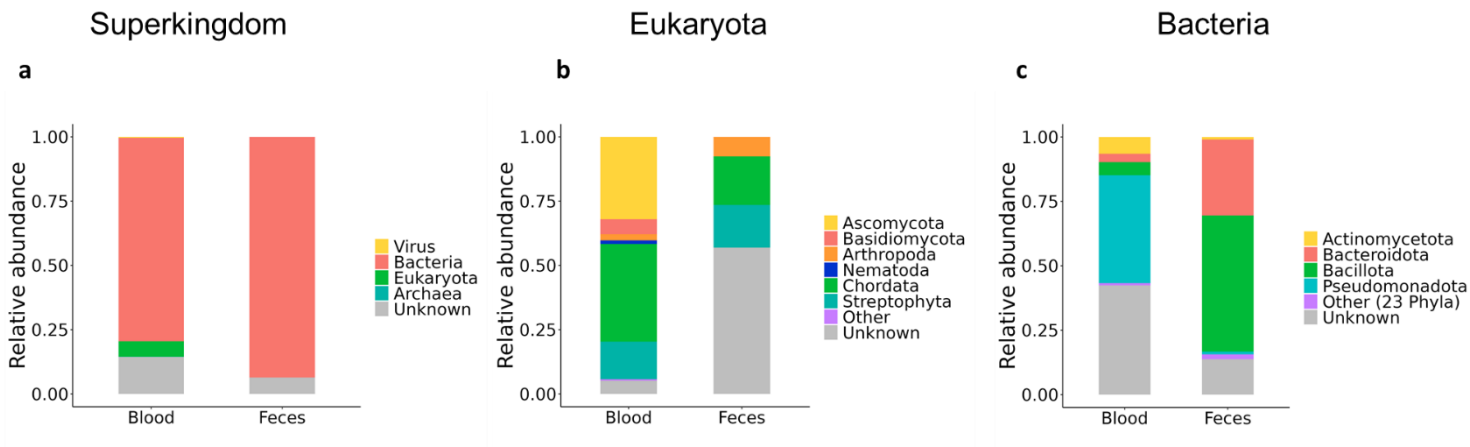

Figure S6: Composition of the non-viral fraction of the samples.
a. Average composition of the non-viral fraction of the samples at the superkingdom level, separated by sample type. **b.** Average compositon of the eukaryotic fraction of the samples at the phylum level, separated by sample type **c.** Average composition of the bacterial fraction of the samples at the phylum level, separated by sample type.

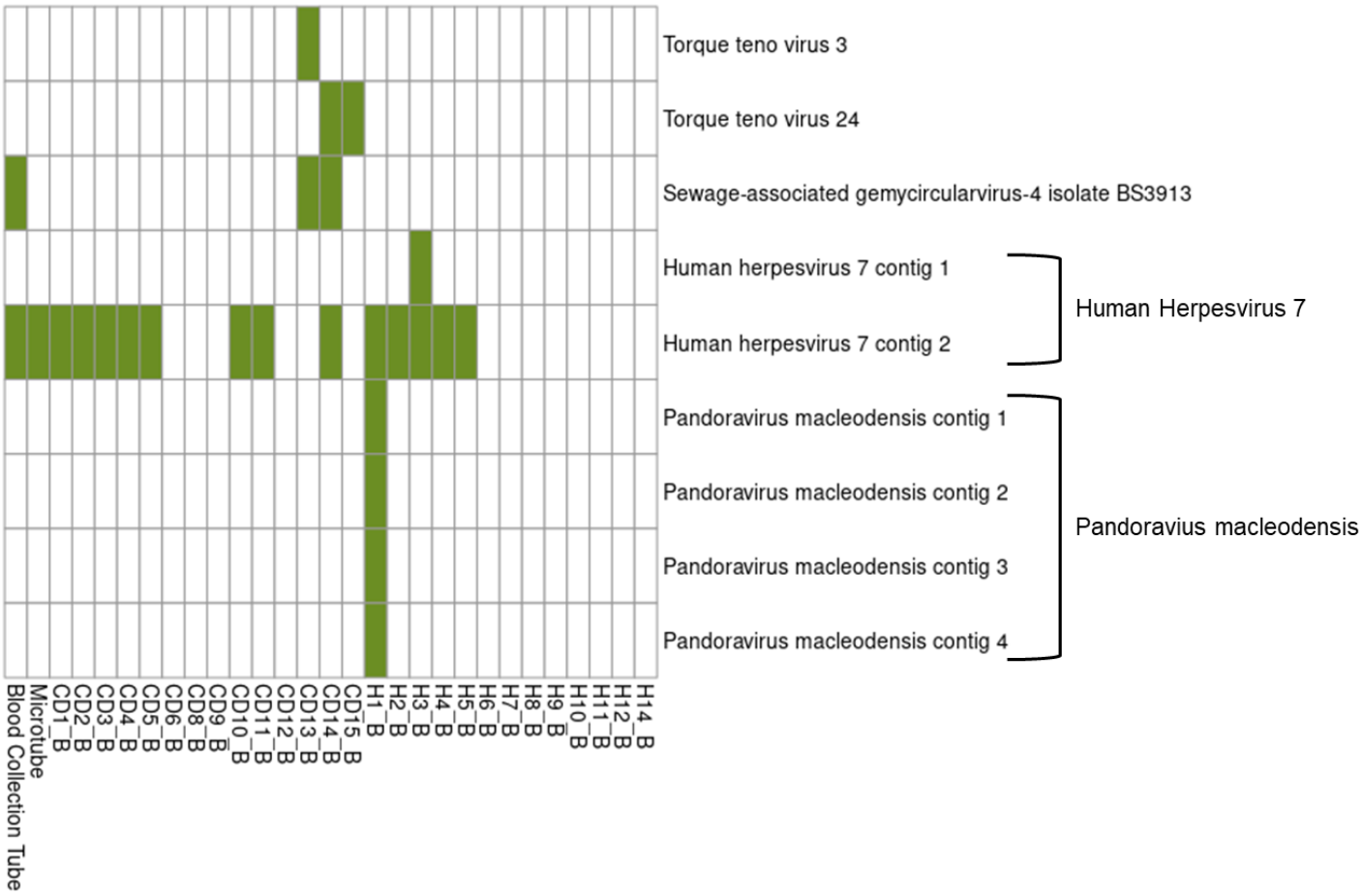

Figure S7: Eukaryotic viruses in blood samples.
Presence/Absence table of the eukaryotic viruses found in the negative controls and in the blood samples.

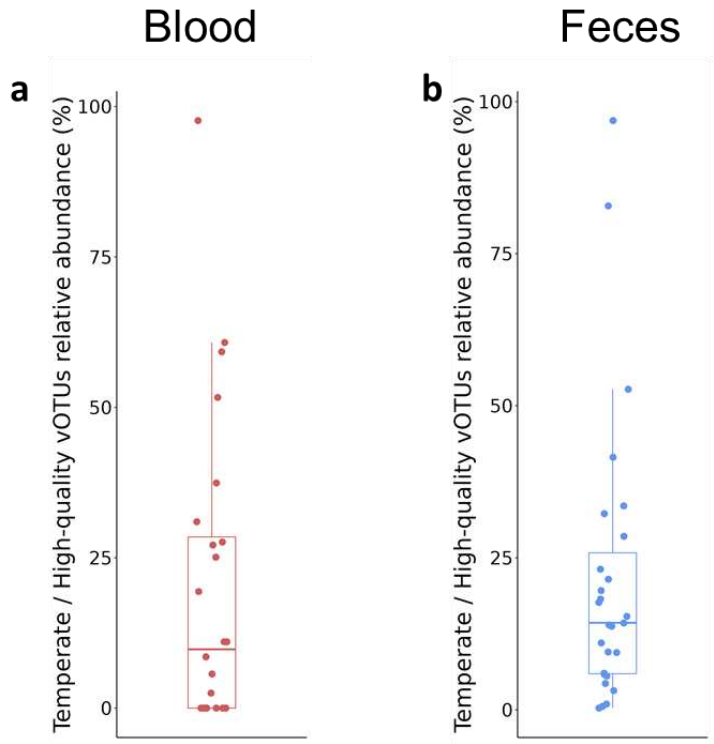

Figure S8: Temperate phage content of blood and fecal samples.
a. Relative abundance of temperate phages among all high quality vOTUs, per blood sample.
b. Relative abundance of temperate phages among all high quality vOTUs, per fecal sample.

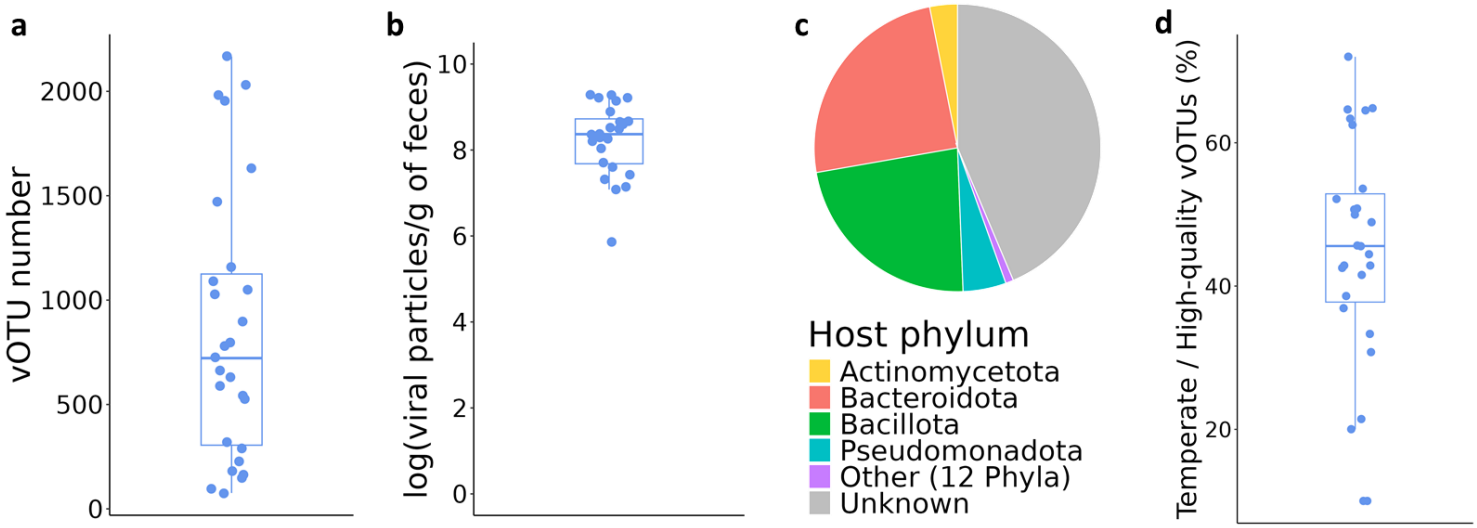

Figure S9: Characteristics of the human fecal virome.
a. Number of vOTUs per fecal sample. **b.** Estimated number of viral particles per g of feces and per fecal sample. **c.** Distribution of the predicted host phyla for all the vOTUs found in fecal samples. **d.** Percentage of vOTUs with a temperate lifestyle among the high-quality vOTUs. The temperate lifestyle was predicted by the presence of genes coding for an integrase, and only the high-quality genomes were considered (Methods).

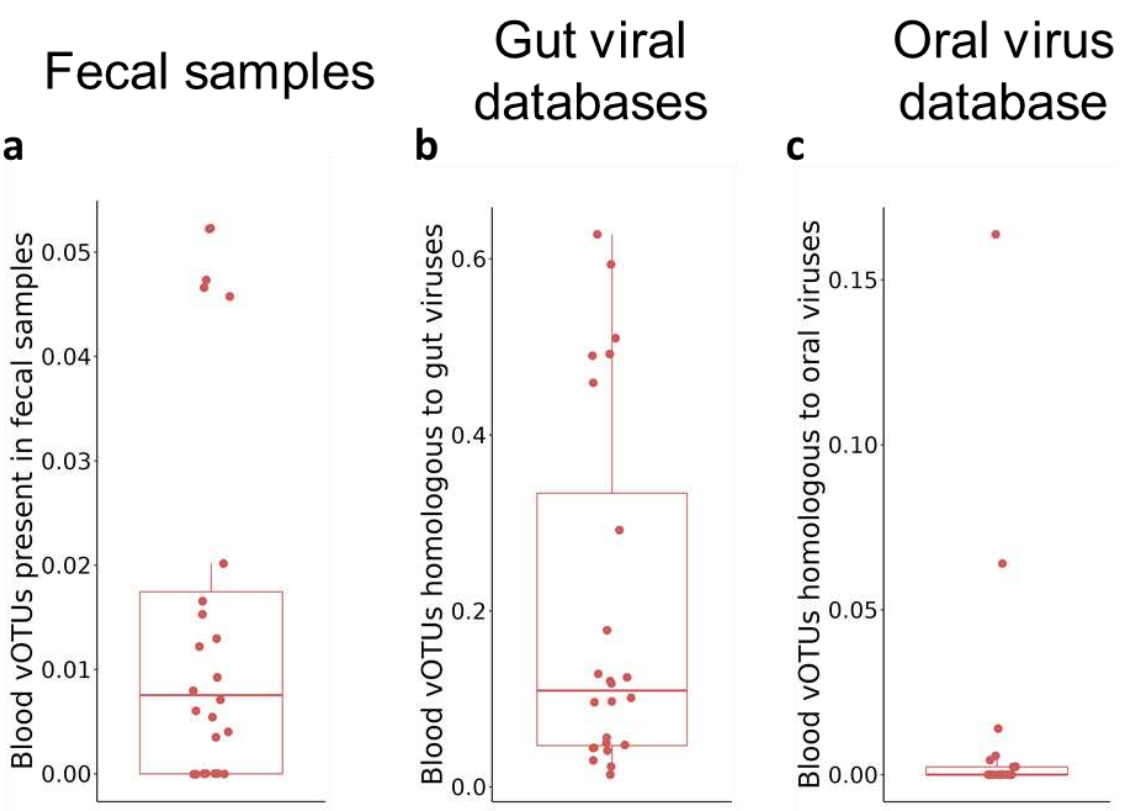

Figure S10: Abundances for the blood vOTUs of different origins.
a. Total relative abundance per blood sample of the vOTUs also found in fecal samples. **b.** Total relative abundance per blood sample of the vOTU homologous to viruses found in gut virus databases. **c.** Total relative abundance per blood sample of the vOTU homologous to viruses found in the Oral Virus Database.

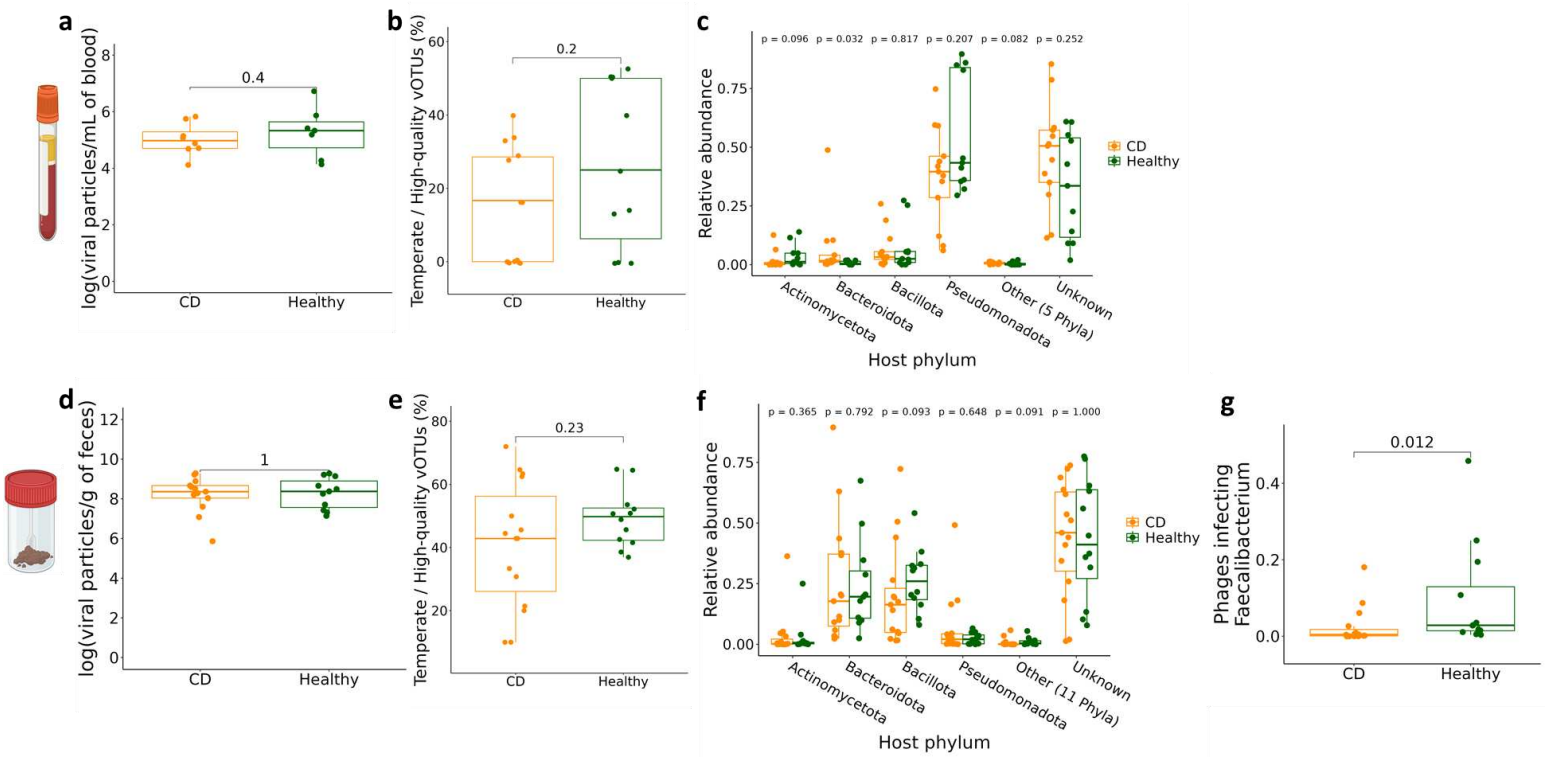

Figure S11: Crohn's disease vs. healthy comparison for blood virome metrics.
a. Estimation of the quantities of viral particles per mL of blood and per blood sample, separated by disease status. **b.** Percentage of vOTUs with a temperate lifestyle among the high-quality vOTUs per blood sample, separated by disease status. The temperate lifestyle was predicted by the presence of genes coding for an integrase, and only the high-quality vOTUs were considered (Methods). **c.** Total relative abundance for each predicted host phylum, per blood sample, separated by disease status. **d.** Estimation of the quantities of viral particles per g of feces and per fecal sample, separated by disease status. **e.** Percentage of vOTUs with a temperate lifestyle among the high-quality vOTUs per fecal sample, separated by disease status. The temperate lifestyle was predicted by the presence of genes coding for an integrase, and only the high-quality vOTUs were considered (Methods). **f.** Total relative abundance for each predicted host phylum, per fecal sample, separated by disease status. **g**. Total relative abundance for all phages predicted to infect the genus *Faecalibacterium*, per fecal sample, separated by disease status.

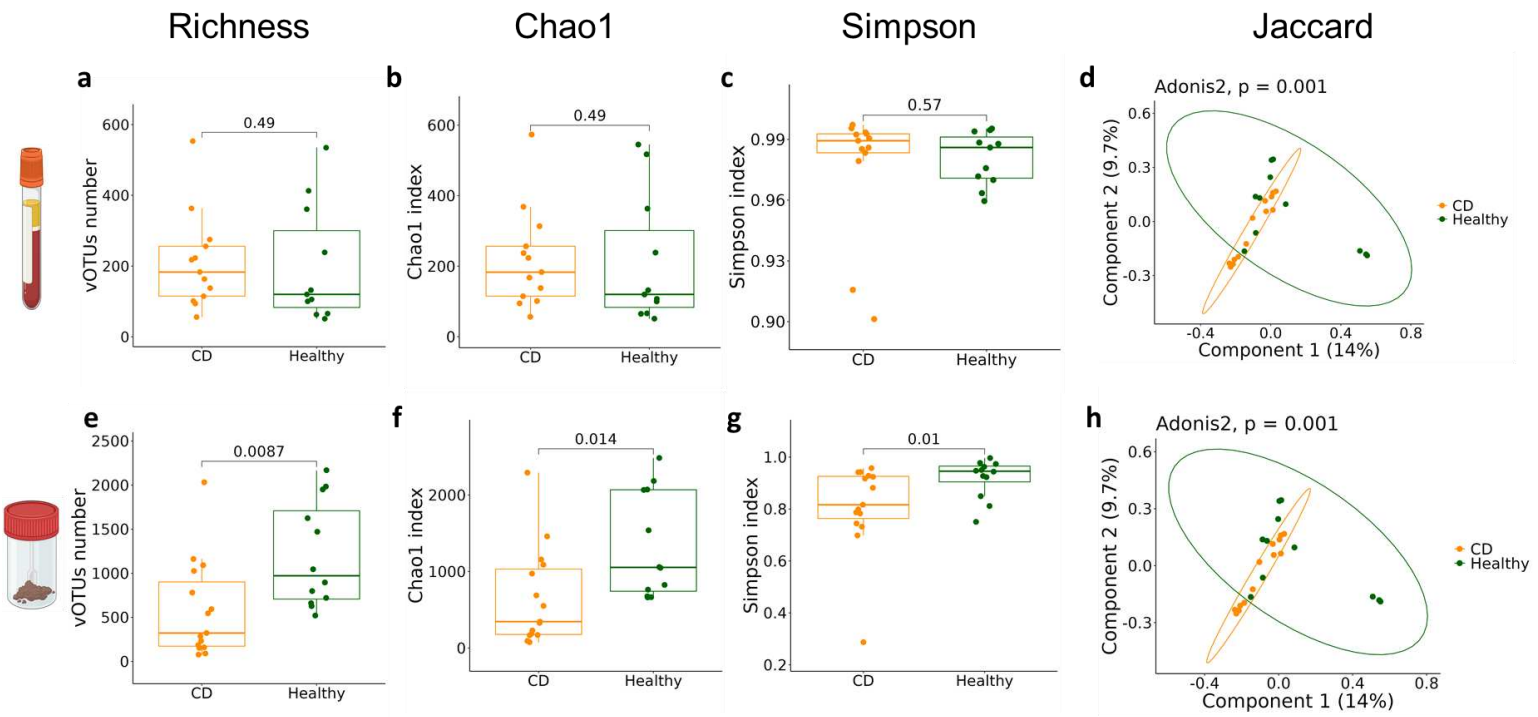

Figure S12: Additional alpha and beta diversity measurements for the blood and fecal viromes.

a. Number of vOTUs per blood sample, separated by disease status. **b.** Alpha diversity, measured by the Chao1 index for the blood samples, separated by disease status. **c.** Alpha diversity, measured by the Simpson index for the blood samples, separated by disease status. **d.** PCoA of the vOTU composition of the fecal samples, using Jaccard distances. The associated Adonis2 analysis revealed a difference between both groups (p=0.001). **e.** Number of vOTUs per fecal sample, separated by disease status. **f.** Alpha diversity, measured by the Chao1 index for the feces samples, separated by disease status. **g.** Alpha diversity, measured by the Simpson index for the fecal samples, separated by disease status. **h.** PCoA of the vOTU composition of the fecal samples, using Jaccard distances. The associated Adonis2 analysis revealed no significant difference between both groups (p=0.492).

Supplementary Tables

Individual	Sampling date	Sex	Age	Age at diagnosis	Localisation (Montreal)	Flare/Remission	C-reactive protein (mg/L)	Harvey-Bradshaw Index	smoking	Surgery	Antibiotics (last 3 months)	Undergoing treatment
CD1	29/02/2020	Female	53	37	L2	Remission	1	2	Past	No	No	Yes
CD2	2020	Female	40	NA	E3	Remission	1	NA	Past	No	No	No
CD3	2020	Female	38	NA	L3L4	Flare	1	4	Never	No	No	No
CD4	2020	Male	44	NA	L3L4	Remission	0.6	1	Never	No	No	No
CD5	13/08/2020	Female	40	20	L3	Remission	5	2	Past	No	No	Yes
CD6	15/09/2020	Male	60	55	L3	Flare	5	7	Never	No	No	Yes
CD7	24/05/2019	Female	26	16	L3	Flare	89.9	NA	Past	No	No	No
CD8	10/07/2020	Male	42	13	L3	Flare	6.3	3	Never	No	No	Yes
CD9	06/07/2020	Male	47	12	L2	Remission	7.8	0	Past	No	No	No
CD10	31/05/2018	Female	50	47	L1	Remission	1	NA	Current	No	No	Yes
CD11	21/06/2020	Female	33	19	L3	Flare	5.3	NA	Past	No	No	No
CD12	03/07/2020	Male	22	20	L3	Remission	5	3	Never	No	No	Yes
CD13	16/06/2020	Male	56	52	L1	Flare	8.7	7	Past	No	No	Yes
CD14	26/10/2020	Female	56	20	L3	Remission	1	2	Never	No	No	Yes
CD15	02/10/2020	Female	37	27	L3	Flare	1	7	Past	No	No	No
H1	2020	Female	26	NA	NA	NA	NA	NA	Never	No	No	No
H2	2020	Female	28	NA	NA	NA	NA	NA	Never	No	No	No
H3	2020	Male	31	NA	NA	NA	NA	NA	Never	No	No	No
H4	2020	Male	29	NA	NA	NA	NA	NA	Never	No	No	No
H5	2020	Male	36	NA	NA	NA	NA	NA	Never	No	No	No
H6	2021	Female	25	NA	NA	NA	NA	NA	Current	No	No	No
H7	2021	Male	32	NA	NA	NA	NA	NA	Never	No	No	No
H8	2021	Female	38	NA	NA	NA	NA	NA	Current	No	No	No
H9	2021	Female	27	NA	NA	NA	NA	NA	Never	No	No	No
H10	2021	Female	29	NA	NA	NA	NA	NA	Never	No	No	No
H11	2021	Female	56	NA	NA	NA	NA	NA	Never	No	No	No
H12	2021	Female	41	NA	NA	NA	NA	NA	Never	No	No	No
H13	2021	Female	28	NA	NA	NA	NA	NA	Never	No	No	No
H14	2021	Female	55	NA	NA	NA	NA	NA	Never	No	No	No

Table S1: Detailed information about the individuals included in the study.

SampleName	Status	Sample Type	Raw	Clean and non-human	Accession n°
H1_F	Healthy	Feces	4 557 777	3 302 598	
H2_F	Healthy	Feces	5 141 556	3 538 237	
H3_F	Healthy	Feces	4 575 463	3 314 041	
H4_F	Healthy	Feces	5 006 463	3 702 841	
H5_F	Healthy	Feces	6 630 408	4 868 696	
H6_F	Healthy	Feces	6 043 597	4 533 278	
H7_F	Healthy	Feces	149	113	
H8_F	Healthy	Feces	12 607 586	10 702 899	
H9_F	Healthy	Feces	4 957 375	4 008 417	
H10_F	Healthy	Feces	161	122	
H11_F	Healthy	Feces	47 423 047	36 124 946	
H12_F	Healthy	Feces	3 848 503	3 021 191	
H13_F	Healthy	Feces	3 944 094	3 101 396	
H14_F	Healthy	Feces	10 220 371	8 099 646	
CD1_F	Crohn	Feces	3 398 455	2 610 231	
CD2_F	Crohn	Feces	11 438 302	8 205 616	
CD3_F	Crohn	Feces	27 092 512	19 524 928	
CD4_F	Crohn	Feces	18 270 751	12 128 024	
CD5_F	Crohn	Feces	8 453 588	5 729 131	
CD6_F	Crohn	Feces	4 522 582	3 789 808	
CD7_F	Crohn	Feces	2 985 683	2 478 116	
CD8_F	Crohn	Feces	10 219 909	8 279 831	
CD9_F	Crohn	Feces	7 091 001	5 360 552	
CD10_F	Crohn	Feces	9 143 203	7 378 428	
CD11_F	Crohn	Feces	9 290 609	7 084 801	
CD12_F	Crohn	Feces	6 350 692	5 222 735	
CD13_F	Crohn	Feces	7 983 876	6 487 386	
CD14_F	Crohn	Feces	636 447	498 993	
CD15_F	Crohn	Feces	3 500 715	2 724 997	
H1_B	Healthy	Blood	25 145 743	6 790 645	
H2_B	Healthy	Blood	13 872 445	5 336 467	
H3_B	Healthy	Blood	17 469 863	6 122 420	
H4_B	Healthy	Blood	16 038 090	3 433 116	
H5_B	Healthy	Blood	19 342 807	5 840 315	
H6_B	Healthy	Blood	1 916 528	185 563	
H7_B	Healthy	Blood	2 347 924	837 299	
H8_B	Healthy	Blood	2 733 222	788 996	
H9_B	Healthy	Blood	2 689 347	723 438	
H10_B	Healthy	Blood	2 486 126	573 092	
H11_B	Healthy	Blood	1 397 921	160 240	
H12_B	Healthy	Blood	3 711 044	691 480	
H13_B	Healthy	Blood	2 312 559	68 548	
H14_B	Healthy	Blood	5 506 340	2 713 132	
CD1_B	Crohn	Blood	25 941 062	8 696 199	
CD2_B	Crohn	Blood	14 183 825	8 720 837	
CD3_B	Crohn	Blood	29 669 303	14 833 794	
CD4_B	Crohn	Blood	20 129 214	11 955 938	
CD5_B	Crohn	Blood	16 967 073	10 236 927	
CD6_B	Crohn	Blood	4 631 975	1 917 021	
CD7_B	Crohn	Blood	2 048 220	12 333	
CD8_B	Crohn	Blood	7 197 457	3 434 820	
CD9_B	Crohn	Blood	6 813 381	3 293 988	
CD10_B	Crohn	Blood	6 542 891	3 338 429	
CD11_B	Crohn	Blood	7 374 010	2 778 364	
CD12_B	Crohn	Blood	9 614 014	4 117 958	
CD13_B	Crohn	Blood	5 606 138	2 207 758	
CD14_B	Crohn	Blood	5 555 652	2 052 908	
CD15_B	Crohn	Blood	8 436 207	4 380 873	
Microtube			5 242 956	2 930 415	
BloodCollectionTube			10 853 654	4 427 872	

Table S2: **Number of read pairs per sample.**

The number of pairs obtained after sequencing is indicated in the "Raw" column. The number of pairs remaining after quality-filtering and removal of non-human reads is in indicated in the "Clean and non-human" column. The samples with less than 100 000 pairs of clean and non-human reads, highlighted in red, were excluded from the analysis.

Table S3 is too large to be included in a PDF file.

Table S3: Characteristics of all the vOTUs.

The table includes quality, length, annotation, classification, host prediction, homology with oral and gut viral databases for each vOTU. The table is organized as follows: first the non-contaminant vOTUs, those found in blood samples then in fecal samples, and then the contaminant vOTUs (no particular order).